



Robotic bronchoscopy in diagnosing lung cancer—the evidence, tips and tricks: a clinical practice review

Elliot Ho^{1^}, Grady Hedstrom^{2^}, Septimiu Murgu^{2^}

¹Division of Pulmonary & Critical Care Medicine, Interventional Pulmonology, Department of Medicine, Loma Linda University, Loma Linda, CA, USA; ²Division of Pulmonary & Critical Care Medicine, Interventional Pulmonology, Department of Medicine, The University of Chicago, Chicago, IL, USA

Contributions: (I) Conception and design: All authors; (II) Administrative support: None; (III) Provision of study materials or patients: None; (IV) Collection and assembly of data: All authors; (V) Data analysis and interpretation: All authors; (VI) Manuscript writing: All authors; (VII) Final approval of manuscript: All authors.

Correspondence to: Elliot Ho. Division of Pulmonary & Critical Care Medicine, Interventional Pulmonology, Department of Medicine, Loma Linda University, 11234 Anderson St., Loma Linda, CA 92354, USA. Email: eho@llu.edu.

Abstract: The development of robotic-assisted bronchoscopy has empowered bronchoscopists to access the periphery of the lung with more confidence and promising accuracy. This is due in large to the superior maneuverability, further reach, and stability of these technologies. Despite the advantages of robotic bronchoscopy, there are some drawbacks to using these technologies, such as the loss of tactile feedback, the need to overcome computed tomography (CT)-to-body divergence, and the potential for overreliance on the navigation software. There are currently two robotic bronchoscopy platforms on the US market, the Monarch™ Platform by Auris Health® (Redwood City, CA, USA) and the Ion™ endoluminal robotic bronchoscopy platform by Intuitive Surgical® (Sunnyvale, CA, USA). In this clinical practice review, we highlight the evidence and strategies for successful clinical use of both robotic bronchoscopy platforms for pulmonary lesion sampling. Specifically, we will review pre-procedural considerations, such as procedural mapping, room set-up and anesthesia considerations. We will also review the technical aspects of using the robotic bronchoscopy platforms, such as how to compensate for the loss of tactile feedback, optimize visualization, use of ancillary technology to accommodate for CT-to-body divergence, employ best practices for sampling techniques, and utilize information from rapid on-site evaluation (ROSE) to aid in improving diagnostic yield.

Keywords: Robotic bronchoscopy; navigational bronchoscopy; pulmonary nodules; lung cancer

Submitted Jun 13, 2022. Accepted for publication Dec 09, 2022. Published online Jan 09, 2023.

doi: 10.21037/atm-22-3078

View this article at: <https://dx.doi.org/10.21037/atm-22-3078>

Introduction

Bronchoscopy is the preferred technique in the evaluation of parenchymal pulmonary lesions (PPL) in patients with suspected lung cancer. This is because bronchoscopic sampling and endobronchial ultrasound (EBUS) evaluation of the mediastinal, hilar and interlobar lymph nodes for

lung cancer staging can take place in the same procedure.

Historically, bronchoscopic sampling of PPL comprised navigating through distal airways with a flexible bronchoscope towards the target lesion by using a computed tomography (CT) scan of the chest as the frame of reference. This not only required proficient understanding

[^] ORCID: Elliot Ho, 0000-0003-0333-6709; Grady Hedstrom, 0000-0002-4961-2767; Septimiu Murgu, 0000-0003-1830-1744.

of the distal airway anatomy, but was challenging due to the limited maneuverability of the conventional bronchoscope and the inability to directly visualize the nodule at the time of biopsy. Conventional bronchoscopy had demonstrated a rather suboptimal sensitivity (14–63%) for diagnosing malignant lesions and worse for those that are less than 20 mm in diameter (1,2). More recent electromagnetic navigation bronchoscopy (ENB) technologies have increased the ability of the bronchoscopist to sample PPL, however still with reported variable yields. A systematic review and meta-analysis found that the pooled sensitivity of ENB was 77%, with most studies being done with the superDimension[®] system (3).

The development of robotic-assisted bronchoscopy (RAB) over the recent years has improved the confidence in the ability to navigate to PPL safely and reliably. This is due in large to the superior maneuverability, further reach, and stability of these technologies (4-8). The use of RAB platforms for PPL sampling have become even more prevalent as more lung nodules are being identified due to the liberalized lung cancer screening guidelines, increasing prevalence of chronic lung disease, and improvements in advanced chest imaging (9). However, the biggest barriers to widespread use of RAB are the cost of the platform, the disposable scopes and tools, as well as the anesthesia and support staff needed for its safe and effective use.

In this article, we aim to review the key published evidence regarding RAB use and highlight strategies for successful clinical use of both RAB platforms for PPL sampling. Specifically, we will discuss the approach to procedural mapping, room set-up and anesthesia considerations. We will also review the practical aspects of using the RAB platforms, such as how to compensate for the loss of tactile feedback, optimize visualization, use of ancillary technology to account for CT-to-body divergence, employ best practices for sampling techniques, and utilize information from rapid on-site evaluation (ROSE) to aid in improving diagnostic yield.

Methods

To identify all landmark studies on ENB and RAB published over the last 20 years, from June 1st, 2002 through June 1st, 2022, we performed a PubMed search using different combinations of the following search terms: “robotic bronchoscopy”, “robotic assisted bronchoscopy”, “navigational bronchoscopy”, “electromagnetic navigation”,

“fluoroscopy”, “radial endobronchial ultrasound”, “transbronchial lung biopsy”, “peripheral pulmonary lesion”, “lung nodule”, and “lung cancer”. Additional papers were identified by reviewing reference lists of relevant publications. Publications in non-English languages were excluded. For this clinical practice review, data were extracted based on their relevance to the topic instead of implementing a systematic approach to article selection. More details of the methods are shown in [Table S1](#).

Evidence

There are currently two RAB platforms in the US market, the Monarch[™] Platform by Auris Health[®] (Redwood City, CA, USA) and the Ion[™] endoluminal robotic bronchoscopy platform by Intuitive Surgical[®] (Sunnyvale, CA, USA). Both robotic platforms require physician control to operate and are not “self-driving”. Both systems use a CT-derived airway map to correlate the position of the scope or catheter with the CT-derived map to help the operator navigate to the target lesion. Both robotic platforms improve the precision of bronchoscopic PPL sampling by offering increased stability, further reach, improved maneuverability, and enhanced dexterity.

While there are similarities, the two robotic platforms differ in the inherent technology. The Monarch[™] robotic platform utilizes a proprietary navigation algorithm which fuses optical pattern recognition with electromagnetic positioning and robotic insertion data, to determine the final scope tip position within the lung and corroborates those signals with the CT-derived airway map. The Monarch[™] robotic bronchoscope uses a mother-daughter telescoping design. The outer sheath has a 6.0-mm outer diameter (OD), and the inner bronchoscope has a 4.2-mm OD with a 2.1-mm inner diameter (ID) working channel. The outer sheath provides increased stability, while the flexibility of the inner bronchoscope allows for increased maneuverability and articulation. The Monarch[™] Platform is designed to provide continuous vision throughout the procedure, including the time of lesion sampling.

The Ion[™] robotic platform utilizes proprietary shape-sensing technology applied in the form of a fiber embedded along the robotic catheter to provide real-time shape and location information. This data allows the catheter tip to corroborate with the CT-derived airway map to determine final catheter tip position within the lung. The Ion[™] robotic platform uses a robotic catheter with a 3.5-mm OD

and a 2.0-mm ID working channel. During navigation, a 1.7-mm OD vision probe is inserted via the working channel of the robotic catheter in order to provide direct visualization. However, the vision probe is removed to allow for the insertion of biopsy instruments at time of lesion sampling. Therefore, there is a loss of vision at the time of PPL sampling.

Monarch

The Monarch™ Platform was initially assessed by the REACH trial in 2018 which showed that the robotic platform was able to reach farther than conventional bronchoscopy (9th generation *vs.* 6th generation) in cadaveric models when compared with a 4.2-mm OD flexible bronchoscope (6). A subsequent cadaver trial (ACCESS; 2019) demonstrated a 94% rate of successful navigation and transbronchial needle aspiration (TBNA) in peripherally placed artificial targets (7). The first human use was documented by Rojas-Solano *et al.* in 2018, where they showed that 14 of 15 lesions were sampled successfully (10). The first post-marketing study by Chaddha *et al.* yielded similar results, quoting 88.6% navigational success based on radial endobronchial ultrasound (r-EBUS) confirmation, with a diagnostic yield range of 69.1–77%, depending on the labeling of inflammatory changes as non-diagnostic or diagnostic specimens, respectively (5).

The BENEFIT study was a prospective multi-center trial that enrolled 54 patients from 5 different centers. Median lesion size was 23 mm [interquartile range (IQR), 15–29 mm]. Navigational success was measured by r-EBUS confirmation in 51 of 53 cases (96%). The diagnostic yield, using a very strict definition, was estimated at 74.1% and was stratified by r-EBUS view; 80.6% for concentric and 70% for eccentric views. Complications were comparable to conventional bronchoscopic biopsy, pneumothorax occurred in 3.7% of cases, but chest tube insertion was needed in 1 of 54 patients (1.9%) (4).

In the largest study with 12 months of follow-up published to date, Agrawal *et al.* described factors associated with diagnostic accuracy using the Monarch system in a retrospective cohort study of 124 patients. Median lesion size was 20.5 mm. Navigation success measured by r-EBUS was 82% with a reported diagnostic yield of 77% after 12 months of follow-up (11). Diagnostic yield was similar for concentric (85%) and eccentric lesions (84%) as seen on r-EBUS, which is a paradigm shift in r-EBUS guided bronchoscopy.

Ion

The Ion™ Platform was initially assessed via implanted targets in human cadavers by Yarmus *et al.* This robotic platform was compared to traditional ENB and showed 80% navigational success using Ion™ *vs.* 45% with ENB as measured by needle-in-nodule on CT (8). Fielding *et al.* in 2019 studied Ion™ in 29 human subjects showing navigational success in 96.6% of cases and a diagnostic yield of 79.3% with 6 months of follow-up (12). Benn *et al.* evaluated 52 patients showing a navigational success of 100% with a reported diagnostic yield of 86%, also with 6 months of follow-up (13). Of note, non-specific benign findings such as inflammation and infection were considered diagnostic specimens, which other studies with stricter definitions label as non-diagnostic materials. Furthermore, cone beam CT (CBCT) was used in 100% of cases and adjustments based on CBCT were performed in 15% of cases, making it difficult to assess the true diagnostic value of the robotic system.

Kalchier-Dekel *et al.* in 2022 published a retrospective single-center trial comprised of 130 patients from a tertiary cancer institution with 12 months of follow-up. Median lesion size was 18 mm (IQR, 13–27 mm). Navigational success was quoted as 98.7% as assessed by the software. Radial EBUS was used in 85% of cases with a concentric or eccentric view obtained in 91% of those cases. The overall diagnostic yield was 81.7% which was stratified multiple ways; by r-EBUS view, the diagnostic yield was 93% for concentric and 78.8% for eccentric view. Complication rates were low with two patients requiring intervention for post procedural pneumothorax (14). This study used a strict definition of diagnostic yield, similar to the BENEFIT trial that used the Monarch system (4).

Clinicians and researchers must recognize that there are several definitions of diagnostic yield based on what is considered a benign diagnosis and based on how the study managed patients lost to follow-up (15). These differences partially explain the wide variability in diagnostic yield reported in bronchoscopy studies. In addition, cancer prevalence also affects diagnostic yield, which also explains why studies from cancer institutions tend to show higher yields. This topic will be discussed further in a later section.

Planning strategies

Mental planning

Pre-procedural planning requires thoughtful understanding

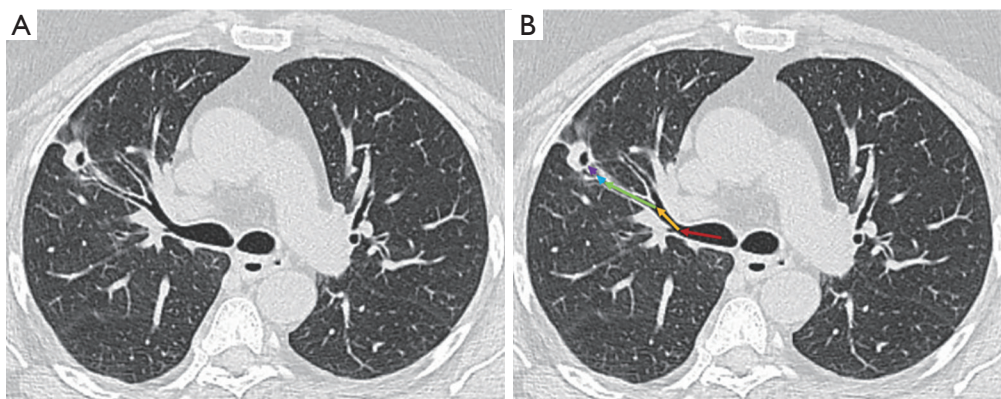


Figure 1 Pre-procedural CT Chest showing a right upper lobe cavitory lesion is used for pathway mapping (A). Review of the CT Chest shows that to arrive at the target lesion, the bronchoscope must navigate via the right main bronchus (red arrow), then the anterior segment (yellow arrow), then take a posterior turn (green arrow), then take one more anterior turn (blue arrow), and lastly potentially another anterior turn (purple arrow) (B). It is important to ensure that there is appropriate understanding of the lesion to airway relationship and writing down this plan prior to the procedure could be useful in cases of CT-to-body divergence. CT, computed tomography.

of the pulmonary segmental anatomy. Even before using the respective proprietary planning software to plan the case, the operator is encouraged to carefully review the CT scan of the chest, identifying the target segment, the airway and pulmonary artery branch in the proximity of the lesion, ensuring that there is appropriate understanding of the lesion-airway/vessel relationship.

It is often helpful to write down the path the bronchoscopist plans to take, starting from the distal trachea to the main bronchus, lobar bronchus, segmental airway, and then subsegmental airways (*Figure 1*), noting the relative anatomical position of each subsequent airway branch in relation to the airway before it. Mentally planning the pathway is useful in cases of significant CT-to-body divergence that can occur during general anesthesia, especially in the lower lobes, prolonged procedures and patients with high body mass index. Mental planning allows operators to navigate to the lesion with the robotic scope ignoring the computer-generated pathway, in the occasions where the software generated pathway is clearly inaccurate or suboptimal.

Pre-procedural software-based planning

During the pre-procedural planning phase, CT of the chest with thin-slice protocol (1-mm cuts) obtained during full inspiration is first imported into the planning platform. The proprietary planning software uses the patient's radiographic anatomy to build a virtual bronchoscopic

image of the tracheobronchial tree. Once segmentation is complete (i.e., identification and highlighting of the airway tree), the bronchoscopist identifies and marks the target lesion. The computer then generates a pathway from the central airway to the target lesion. The bronchoscopist can select the pathway that most closely approaches or directly leads to the target lesion and may manually adjust or extend the computer-generated pathway by adding points along visible airways on the CT chest from the target lesion to the central airway. Multiple pathways to the same target lesion can be planned (*Figure 2*). The bronchoscopists should avoid creating pathways that take sharp turns in the mid and peripheral lung regions, as those are not consistent with subsegmental airway branching. When that happens, either a different segmental airway was planned or a pathway was created through the lung parenchyma (*Figure 3*). Of note, there may be heterogeneity in the generation of virtual airways and navigation maps between navigation platforms as demonstrated in the ATLAS study, which compared airway segmentation and pathway generation in 41 PPL from 25 patients via three different navigation platforms. These differences may affect accurate navigation and biopsy of PPL (16).

Bronchus sign

For lesions in the mid-lung zone, and occasionally for peripheral lesions, the “bronchus sign” is a useful finding to aid in pathway planning. The “bronchus sign” is defined as

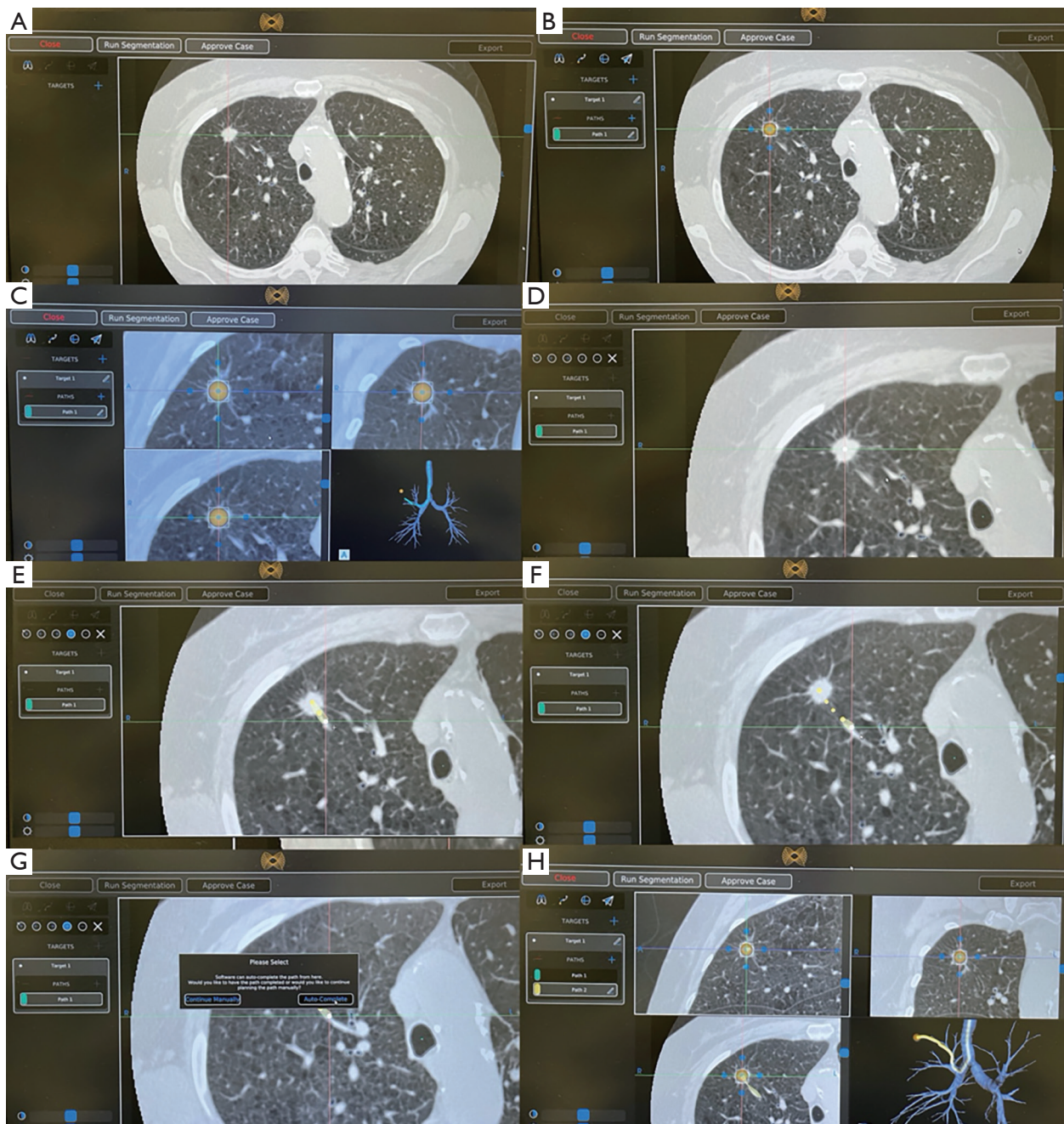


Figure 2 Example of planning a target in the Monarch system software. A target is chosen (A) and marked (B). The software will draw a pathway automatically along segmented airways which in this example is stopping proximal of target itself (C). A pathway can be manually drawn (D) and traced back, in this example along a blood vessel (E,F) until contacting a segmented airway at which point the software will complete the pathway (G). The new pathway is shown leading into the target (H). Generated pathways have to be without sharp angulation, especially in the mid and outer third of the lung (see image H bottom right panel). That ensures that the pathway follows normal structures (airway or vessels) and is not artificially created through the lung parenchyma.

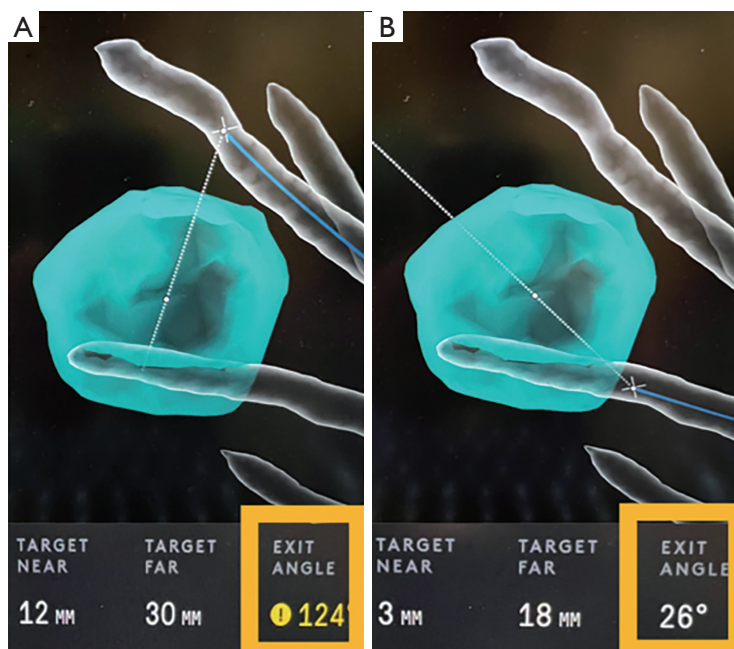


Figure 3 A mapped pathway (blue line) extending to the virtual target is seen on a computer-generated airway tree. Although in close proximity to the virtual target, the mapped pathway (blue line) exits the airway at a very sharp angle as indicated by the high exit angle (yellow box). This is not consistent with subsegmental airway branching (A). A different pathway is mapped towards the virtual target, this time exiting the airway at a more gradual angle as indicated by the low exit angle (yellow box) (B).

the presence of an airway leading directly to a pulmonary lesion. In many, but not all studies, the presence of a “bronchus sign” has been associated with an improvement in diagnostic yield. In a meta-analysis of 2,199 lesions, the diagnostic yield was reported as 74.1% *vs.* 49.6% when a “bronchus sign” was present versus absent (17). In an older ENB study, Seijo and colleagues also reported an increased diagnostic yield of PPL sampling with the presence of a “bronchus sign” as opposed to its absence (79% *vs.* 31%) (18). The increased diagnostic yield of PPL sampling in the presence of a “bronchus sign” has been corroborated by the NAVIGATE trial (19). From the published evidence to date on RAB, two papers showed improved diagnostic yield when a “bronchus sign” is present (5,11), while two papers reported a trend towards improved diagnostic yield but did not show statistical significance (4,14), and two papers did not report on this variable (12,13). Interestingly, a meta-analysis of 51 r-EBUS studies (N=7,601 patients), showed no association between r-EBUS sensitivity for malignancy and bronchus sign, average nodule size, use of fluoroscopy, virtual bronchoscopy, guide sheath, cancer prevalence, multicenter status, or consecutive enrollment.

Only the use of rapid on-site cytology was associated with increased sensitivity in this analysis (20).

Vessel sign

Despite its utility, prior studies have reported that up to 40–60% of cases of guided bronchoscopy lack a “bronchus sign” when undergoing navigational bronchoscopy, especially in patients with emphysema in which the resolution of the chest CT is suboptimal for identifying peripheral airway walls (18,21–23). This is especially true for nodules that are pleural based or reside in the peripheral one-third of the lung. Recognizing that vessels, lymphatics, and airways are adjacent in the bronchovascular bundle, in patients where a vessel (pulmonary artery branch) is seen leading to the target nodule, there is usually also an airway which may not be seen on the CT due to the lack of contrast between the peripheral bronchi and surrounding emphysematous lung parenchyma. The theoretical evidence supporting vessels as a surrogate for an absent “bronchus sign” on CT is well corroborated by developmental biology; blood vessels develop at the same time as airways and

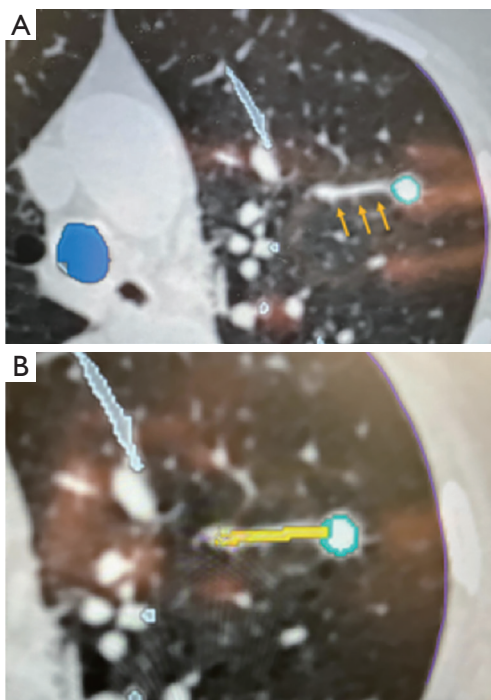


Figure 4 Vessel sign planning in the absence of bronchus sign. Pre-procedural planning CT chest showing the vessel leading to a nodule (yellow arrows) (A). A pathway to the target lesion is created by manually adding points along the vessel from the target lesion to the central airway. This is demonstrated by the yellow pathway from the lesion connecting to the central airway (B). CT, computed tomography.

more specifically, the pulmonary arteries run alongside the airways and the pulmonary veins show a similar branching pattern to the arteries (24,25). By appreciating this finding, the bronchoscopist can manually adjust and extend the computer-generated pathway by adding points along overlapping vessels and then airways from the target lesion towards the central airway (*Figure 4*). In our experience with RAB, we have had success using the “vessel sign” for mapping during pre-procedural planning when a “bronchus sign” is absent (26).

It should be emphasized that the advancement of navigational technology for PPL sampling is not a replacement for experience and thoughtful review of imaging and airway anatomy. Successful planning of a pathway for PPL sampling using these navigation platforms requires appropriate understanding of the tracheobronchial anatomy and comprehension of the lesion to airway relationship. The bronchoscopist should always review the

chest CT prior to the case and take notes of the pathways that lead to the target lesions.

Room set-up

Pre-planned room set up and consideration of ergonomics with respect to equipment, patient, and personnel positioning are relevant for performing a successful robotic bronchoscopy. Set up should ultimately be decided with input from all team members prior to the procedure with consideration to individual room logistics.

General components that must be considered for positioning are the location of the patient on fluoroscopy compatible bed, robotic bronchoscopy tower (in the case of MonarchTM), robotic bronchoscope actuator, anesthesia machine, general bronchoscopy tower, C-arm for fluoroscopy, CBCT (when used), specimen processing station, cytopathology or ROSE station, and location of individual staff members. Usual staff include bronchoscopist +/- assistant, anesthesiologist or certified registered nurse anesthetist, bronchoscopy nurse, bronchoscopy technician, cytopathologist or cytology technician. *Figure 5* illustrates an example of equipment positioning utilizing the MonarchTM system. For ENB-based technologies, like the MonarchTM RAB, it is important to assure removing all metal objects (including the C-arm) from the proximity of the field generator during the registration and navigation parts of the procedure.

Anesthesia considerations

Ventilatory and oxygenation settings possibly affect the success of robotic navigation, sampling, and avoidance of complications. Atelectasis following intubation can alter nodule location, due to changes in lung volumes leading to worsened CT-to-body divergence and may also provide false positive or confusing r-EBUS views. Additionally, collapse of distal airways can lead to loss of vision during navigation. The I-LOCATE trial performed an r-EBUS survey under fluoroscopic guidance in dependent segments of the lung and found that 51 of the 57 patients (89%) had evidence of atelectasis in at least one dependent airway segment and 18 patients (32%) had evidence of atelectasis in 6 segments (27). This problem can be diminished by optimizing certain anesthesia settings, as highlighted below.

Optimal positive end expiratory pressure (PEEP) of 8–10 cmH₂O, or even higher, could splint open distal airways to

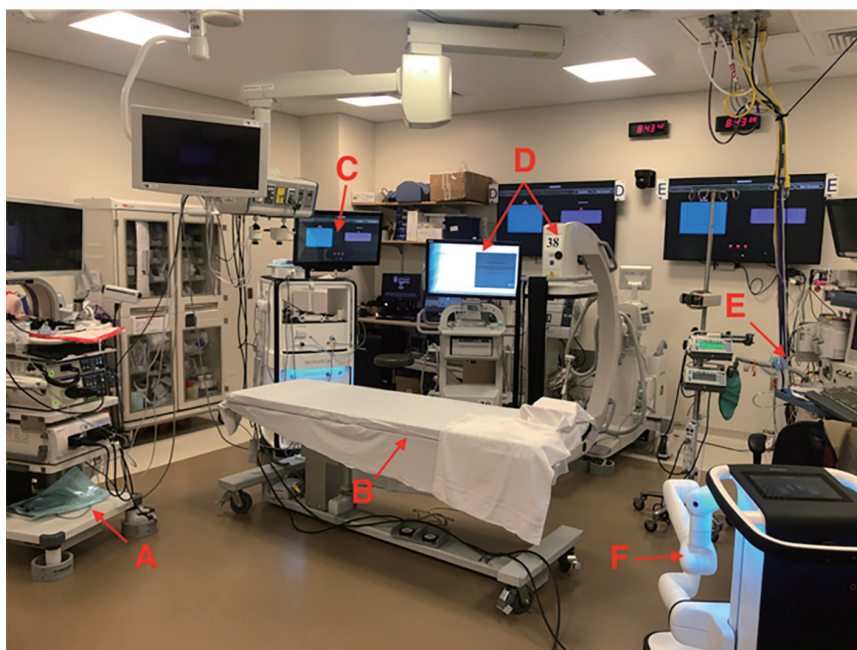


Figure 5 Example of room set up for Monarch™ system. Pictured are bronchoscopy tower (A), fluoroscopy compatible bed (B), Monarch tower (C), C-arm and fluoroscopy tower (D), anesthesia machine (E), and Monarch robotic bronchoscope driver (F). Not pictured are stations for specimen handling, cytopathology/ROSE, and nursing. ROSE, rapid on-site evaluation.

potentially mitigate atelectasis and more closely approximate the conditions of a full inspiratory breath used when the CT images are acquired, thus potentially decreasing CT-to-body divergence. Ideally, application of higher PEEP or a recruitment maneuver (e.g., pressure support of >20 cmH₂O for >20 seconds) should be applied prior to navigation or wedging of the sheath or bronchoscope into the target segment to allow transmission of pressure to the distal airways. A recent study demonstrated that when a ventilation strategy which incorporates recruitment maneuver after endotracheal intubation, followed by fraction of inspired oxygen (FiO₂) titration ($<100\%$) and maintaining PEEP of 8–10 cmH₂O as compared with standard ventilation strategy (no recruitment measure, FiO₂ of 100%, and PEEP of 0 cmH₂O), atelectasis can be reduced from 84.2% to 28.9% ($P<0.0001$) and bilateral atelectasis can be reduced from 71.1% to 7.9% ($P<0.0001$) as documented by CBCT; without increased incidence of pneumothorax or pneumomediastinum (28). Injection of air using a 60-mL syringe (*Figure 6*) can splint the peripheral airways (especially in patients with emphysema and easily collapsible airways) and facilitate advancement of the scope further into the lung. Injection of saline has also been used

to splint open airways and it is more effective than air, however this can confound r-EBUS and CBCT views (as it leads to alveolar filling in the target subsegment) as well as disrupt cells making ROSE interpretations more difficult.

Lower FiO₂ following pre-oxygenation for induction of anesthesia is thought to lead to less atelectasis as well. The effect of FiO₂ on atelectasis has been well established in anesthesia literature and at fractions <0.3 , it is thought to develop over hours rather than minutes (29).

Airway motion during navigation can distort anatomy and contribute to CT-to-body divergence. Additionally, since the Monarch™ system partially relies on airway imaging recognition, airway movement during respiration or due to cardiac pulsations can make navigation less accurate. Our practice is to always keep the scope in the center of the airway and use relatively lower tidal volumes (target of 6–8 mL/kg) than traditional tidal volumes in outpatient surgery with a higher respiratory rate to maintain adequate minute ventilation. These settings minimize airway motion during navigation.

Total intravenous anesthesia (TIVA) is our preferred modality of general anesthesia. Bronchoscopic adaptors are rarely completely air-tight and frequent disconnections

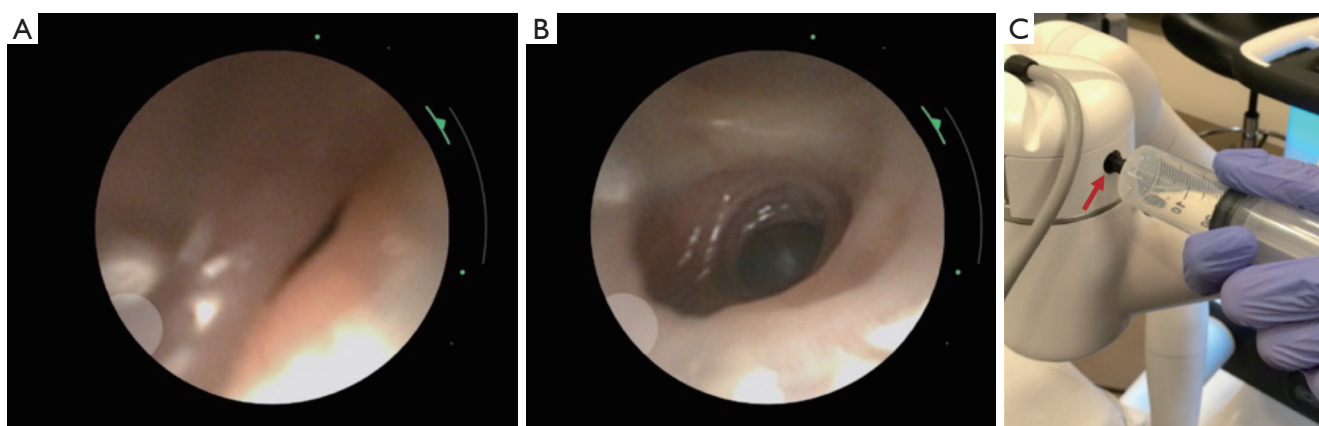


Figure 6 Decreased elastic recoil in COPD; airway collapsibility encountered (A) proximal to the target. Improvement in airway patency (B) is obtained by insufflating air through a 60-mL syringe (C). The proximal valve of the robotic bronchoscope is indicated by the red arrow. COPD, chronic obstructive pulmonary disease.

during set up and take down make use of anesthetic gases less optimal due to their leak into the surrounding environment.

Although guided bronchoscopy has been reportedly performed under moderate sedation, we believe that for RAB, the need for general anesthesia will persist with the current available technology. This is due in large part to the need for a quiet working field during navigation, the ability to adjust PEEP and recruitment maneuvers to splint the airway open, as well as reduction in the respiratory motion to mitigate the amount of CT-to-body divergence. Furthermore, in order to make micro-adjustments when targeting small nodules with the RAB instruments, the patient has to be as still as possible. Any patient movement (such as coughing), can lead to inaccurate localization of the PPL with RAB. This is particularly relevant as we envision the therapeutic potential with RAB (e.g., intralesional chemotherapy, ablation), where a high level of precision and stability is critical. Furthermore, patient movement during RAB can lead to airway trauma, resulting in bleeding and pneumothorax. That being said, if the new generation of robotic scopes are more flexible and receptive to manual commands, it may be possible that RAB can be used with moderate sedation for selected diagnostic procedures.

Navigation and peripheral visualization optimization

Airway inspection

Airway inspection using a conventional or disposable

bronchoscope is typically performed prior to RAB navigation to rule out central endobronchial lesions and aspirate secretions if present. Aspiration of secretions prior to the introduction of the robotic scope is important as this will minimize contamination when sampling and reduce the likelihood of soiling the lens when navigating with the robotic scope. Once the airway assessment and clearance are completed, the robotic bronchoscope is introduced into the endotracheal tube. Unnecessary suctioning should be avoided to prevent atelectasis which can lead to CT-to-body divergence and false positive r-EBUS images, as discussed above. For similar reasons, the inspection bronchoscopy should be short (ideally less than 3 minutes, as atelectasis has been reported as early as 3 minutes post induction of general anesthesia) (27).

Registration

Just prior to navigation, the RAB platform needs to synchronize the position of the robotic bronchoscope with the virtual pathway. During the registration phase with the Monarch™ Platform, the bronchoscope is advanced to the main carina and then retracted back. The computer prompts the operator to advance the bronchoscope to the contralateral main bronchus and then retract once more. This maneuver has to be done smoothly with the scope in the center of the airways. With the Ion™ Platform, registration begins by aligning the distance and rotation of the main carina between the virtual image and live bronchoscopic image. The bronchoscope is driven into

each of the main bronchi, and then driven to the individual lobar and distal airway segments. For both platforms, we recommend that this process is not rushed so that the RAB platform has enough time to pick up as many data points as possible. In the setting of incomplete airway anatomy, such as with pneumonectomy or lobar resection, partial registration can be performed with the IonTM Platform. This can be completed by driving the bronchoscope into bilateral main bronchi, and then to the remaining lobar and distal airway segments (*Figure 7*).

Navigation

Once registration is complete, the virtual image of the tracheobronchial tree with the computer-generated pathway connecting to the target lesion will appear. Using either the handheld controller (MonarchTM Platform) or the track ball and scroll wheel controls (IonTM Platform), the robotic bronchoscope is advanced to the peripheral target by following the pathway that was mapped out during pre-procedural planning.

When navigating the airway, visualization is important to ensure safe passage of the bronchoscope and its instruments without airway trauma. For the MonarchTM system, due to the optical pattern recognition technology, keeping the scope aligned with the airway and avoiding touching the walls or buckling is critical in avoiding navigation errors. This is especially important when accessing the distal airways where the airway anatomy may not always be clear on CT imaging. It is important to remember to navigate with the live bronchoscopic image while using the pathway on the virtual image as a guide. As previously mentioned, successful navigation to the target lesion requires thoughtful review of imaging and appropriate understanding of the tracheobronchial anatomy. When the computer-generated pathway does not correlate with what is seen on the live bronchoscopic view, the bronchoscopists should refer to the CT images and their mental planning, as discussed above.

Compensating for the loss of tactile feedback

When operating any of the RAB platforms, there is a loss of tactile feedback which could theoretically lead to airway trauma followed by pneumothorax or airway bleeding. The MonarchTM system provides “buckling errors” when pressure is applied on the airway walls. We recommend, however, that operators always follow the airway anatomy displayed in real time. Over-emphasis on following the

virtual pathways can lead to airway trauma, especially as vision may be lost in the distal airways. With the RAB platforms, trauma can be mitigated by the presence of visual displays that indicate the articulation tension, torque, and drive force surrounding the robotic scope (*Figure 8*). It is important to pay close attention to these variables when driving and avoid significant strain on the robotic scope.

Optimizing visualization during peripheral navigation

Soiling of the lens during the procedure can pose a challenge to the operator. This can be mitigated by flushing air or small amount of saline through the working channel (for the MonarchTM), gently wiping the lens on the bronchial mucosa, or removing the scope entirely out of the system to clean the lens with an alcohol swab and re-start the registration and navigation process. Although flushing the working channel with saline may help clean the lens, this should be avoided when navigating the distal airways as this may interfere with subsequent r-EBUS imaging and compromise Diff-Quik staining. The operator is also encouraged to avoid suctioning unless absolutely necessary as this may potentially lead to airway trauma, more collapsibility, and worsened vision. Even though airway trauma should be avoided, contact with the airway is sometimes relied upon to manipulate the bronchoscope across the bends of distal carinas and traverse into the distal airways.

Recruitment maneuvers and increased PEEP during navigation but prior to wedging the sheath/scope can be employed to improve patency of distal airways. The use of low tidal volumes can reduce motion, especially when accessing a target lesion in the lower lobes, where the CT-body divergence is most pronounced. When encountering airway collapse of the distal airways, air can be injected via the working channel to retain airway patency. At times, patency of distal airways may be restored by opening the proximal valve of the robotic bronchoscope (*Figure 6C*) to equilibrate the pressures within the distal airways with outside atmospheric pressure. Some operators connect oxygen tubing and instilling continuous low O₂ flow during navigation for a more continuous airway splinting.

Airway splinting techniques with increased pressure support and PEEP are only useful until the sheath (for MonarchTM) or the scope (for IonTM) is wedged into the segmental/subsegmental airways. From then on, the positive pressure ventilation does not affect the target segment and in fact, in the absence of collateral ventilation, may lead

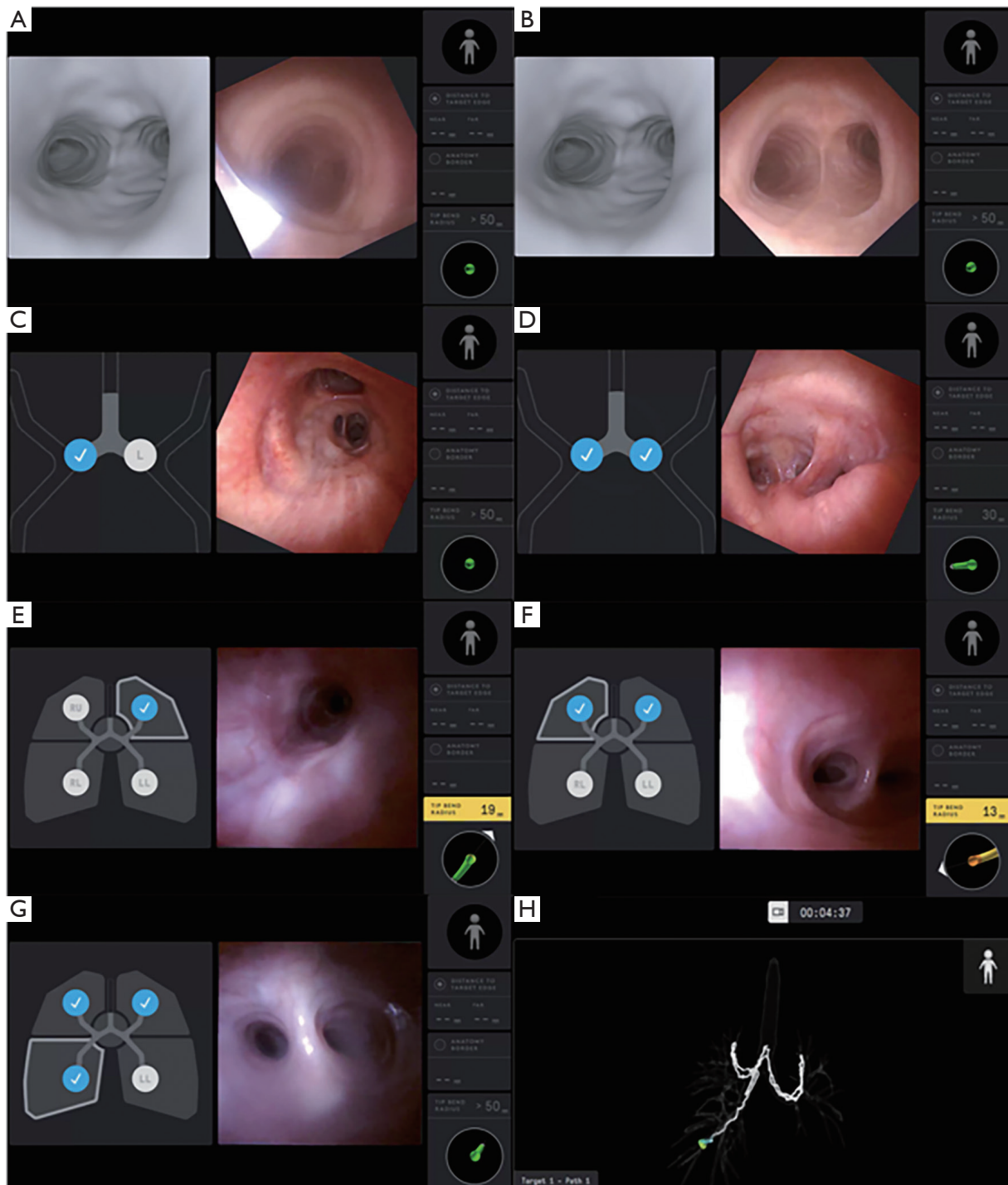


Figure 7 Registration process with the Ion robotic bronchoscopy platform using partial registration in a patient with left lower lobe resection. The robotic catheter and vision probe enter the endotracheal tube into the trachea above the main carina (A). The live image (right panel) is rotated counter-clockwise to align with the virtual image (left panel) (B). The robotic catheter is advanced into the right main bronchus (C), the left main bronchus (D), the left upper lobe (E), the right upper lobe (F), and the right lower lobe (G). A schematic of all the data points gathered during the registration process is seen on a virtual tracheobronchial tree overlay (H).

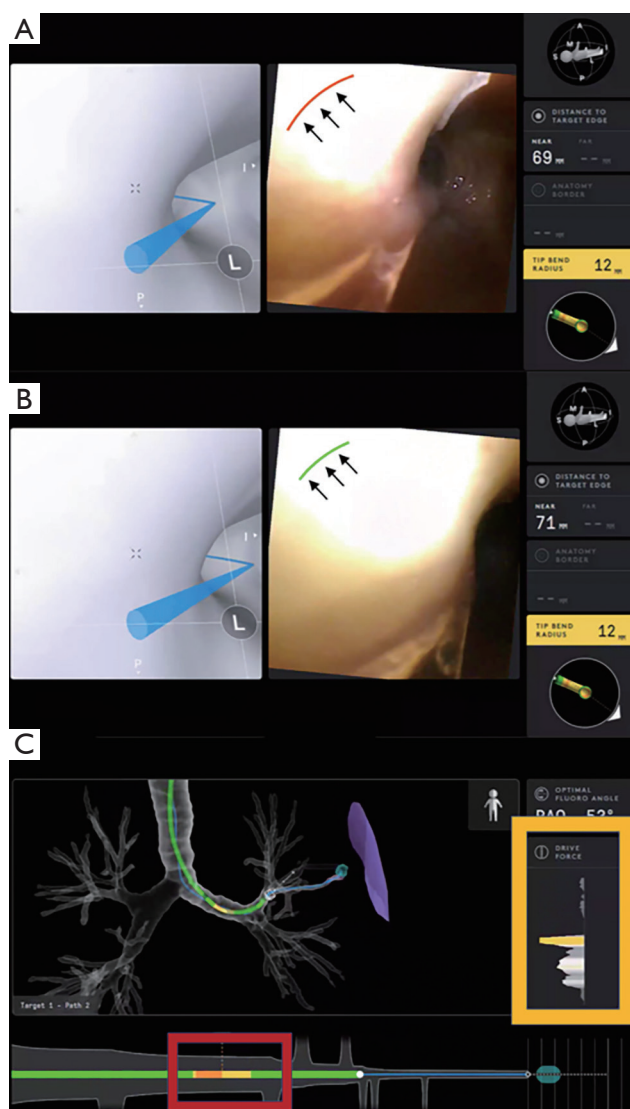


Figure 8 Endoluminal view with the Ion robotic bronchoscopy platform during navigation. The amount and direction of pressure applied by the robotic catheter onto the surrounding airway wall is indicated by the red curved line at the 11 o'clock position (black arrows) (A). The pressure is lessened by moving the robotic catheter away in the opposite direction, as indicated by the green curved line at the 11 o'clock position (black arrows) (B). The amount of pressure applied onto the anterior aspect of the robotic catheter is indicated by the drive force (yellow box), and the amount of tension along different points of the robotic catheter is indicated by different colors (red box) (C).

to overinflation of the adjacent segments and potentially worsening atelectasis in the segment of interest. Once the sheath or the scope is wedged, we return to normal

ventilatory settings. For the Monarch™ system, air or saline insufflation can be introduced through the working channel of the scope throughout the procedure to splint the distal airways. For the Ion™ system, air or saline insufflation can be introduced via the side port of the robotic catheter or directly through the working channel once the vision probe is removed.

Navigating with the Monarch™ Platform

A feature unique to the Monarch™ Platform is the telescoping design of the robotic system (sheath/scope). The capacity to manipulate the outer sheath and inner scope independently allows the operator the ability to maximize on the stiffness of the outer sheath while preserving the flexibility of the inner scope. The “leapfrog technique” uses the junction of the outer sheath and inner scope as a fulcrum to increase the dexterity and maintain control over the robotic scope. By driving the flexible scope into an airway followed by advancing the sheath over the scope in an alternating fashion, the robotic scope can be maneuvered across tight bends which are typically present in the upper lobes and superior segments (*Figure 9*). It is advisable to park the sheath in the segmental or sub-segmental airways. As illustrated in a later section, this may help decrease the rate of pneumothorax and prevent the spillage of blood into a separate airway segment when airway bleeding is present. Lastly, with the Monarch™ system, due to the presence of continuous vision, biopsy instruments can be directed into distal airways and used as a guide sheath for the operator to advance the robotic scope over. This is especially helpful when manipulating past tortuous distal airways. However, the maneuver must be carefully performed to avoid airway trauma at the minor distal carinas.

Navigating with the Ion™ Platform

There are a few features that are unique to the Ion™ Platform which can be helpful at the time of navigation. The Ion™ Platform has an endoluminal compass which is present on the virtual image that indicates the anatomical position of the airway in relation to the patient (*Figure 10*). This function can be especially helpful for the operator to decide how to make fine adjustments to the bronchoscope in relation to the airway wall when advanced imaging, such as augmented fluoroscopy and CBCT, is used in conjunction with the RAB. The “preview path” function is a feature that allows the operator to decouple the virtual image from the

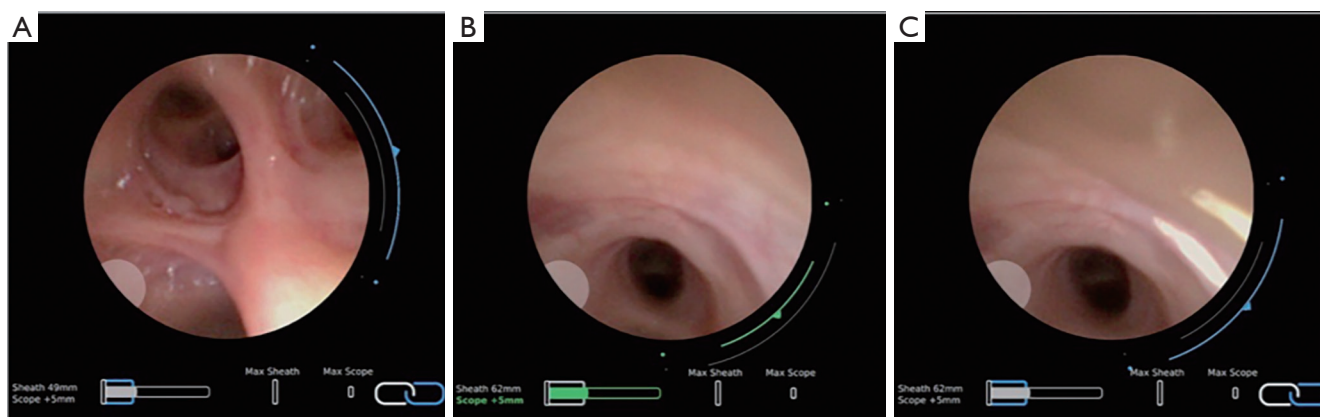


Figure 9 Leapfrog technique to navigate to apical segment of RUL. Sheath is in the RUL but unable to advance it in the RB1 (apical segment) despite maximum articulation; see blue line expanding to the two dots (A). After decoupling, the scope is advanced in RB1 (B). Then the scope and the sheath are recoupled, and the sheath is now in the RB1 segment (C). Navigation is then continued in the scope mode. RUL, right upper lobe.

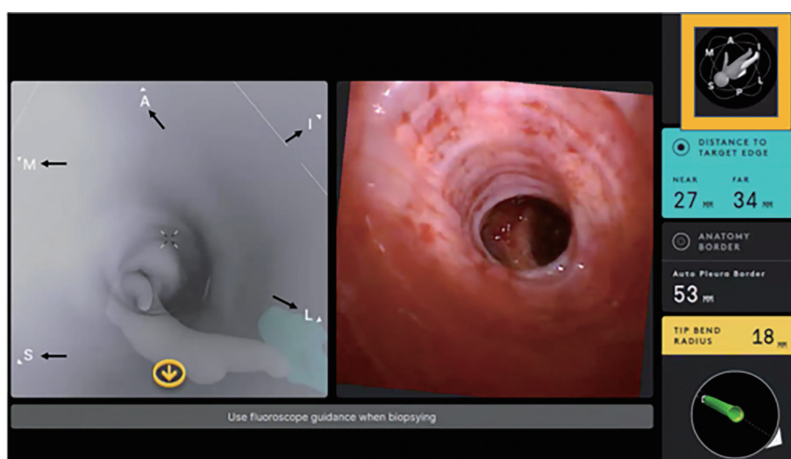


Figure 10 The endoluminal compass is a useful feature on the Ion robotic bronchoscopy platform that helps correlate the position of the robotic catheter in relation to the patient's airway anatomy and target lesion. Letters (black arrows) are seen on the virtual image (left panel), which indicate the respective anatomic positions (A = anterior, I = inferior, L = lateral, P = posterior, S = superior, M = medial). The positional relationship between the robotic catheter and the patient's airway anatomy is also depicted on a 3D figurine (yellow box). 3D, three-dimensional.

live view, and “preview” the virtual path by scrolling distally on the virtual pathway. By “previewing” the virtual pathway, the operator can anticipate upcoming airway branches that are short, sharp, and tortuous, which can be present especially in the distal airway segments. The “preview path” function can also serve as a guide when the operator decides to manually navigate in the presence of significant CT-to-body divergence or rotational-torque to the robotic scope. The operator can advance the robotic scope in a stepwise

fashion and realign the virtual image with the live image at each branch point, while following the mapped pathway (Figure 11).

Confirmation of successful navigation

Troubleshooting CT-to-body divergence

Due to the differences in lung volume at the time of the pre-

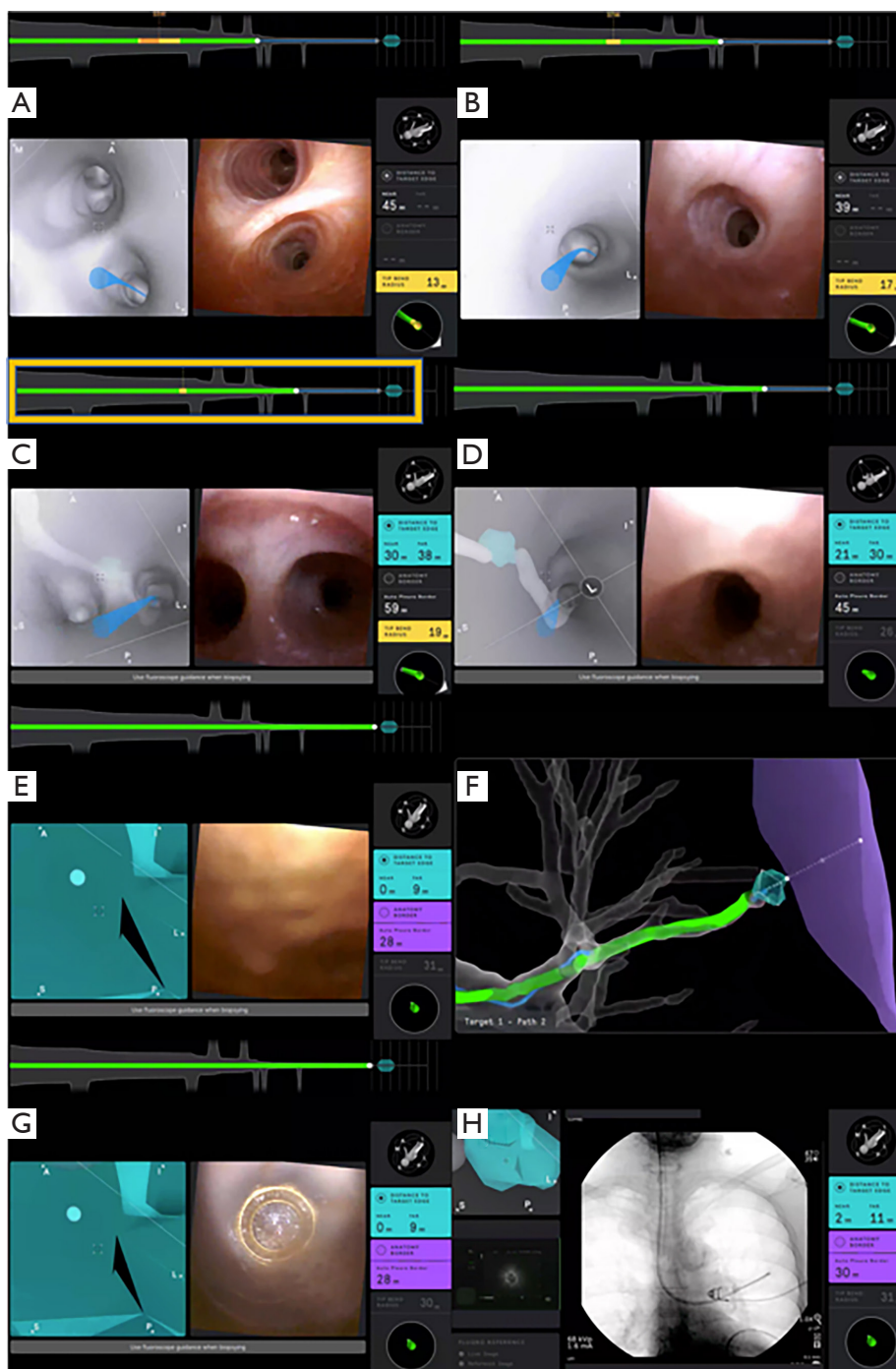


Figure 11 Example of navigation with the Ion™ system. The live image (right panel) correlates with the virtual image (left panel). The blue line indicates the mapped pathway leading to the target lesion (A). The robotic catheter is advanced distally, following the blue line (B). As the robotic catheter is advanced distally, the operator should make sure that the live and virtual images match. Of note, the schematic above the live and virtual images (yellow box) indicates whether the robotic catheter is following or deviating from the planned pathway (C). The virtual target comes into view as the robotic catheter is advanced further following the mapped pathway (D). The robotic catheter is seen adjacent to the target lesion (E). Virtual tracheobronchial tree overlay demonstrates successful navigation to the target lesion (F). The vision probe is retracted slightly within the robotic catheter, showing that it is tented well against the airway mucosa (G). The vision probe is removed from the robotic catheter and replaced with the r-EBUS probe. An eccentric image on r-EBUS is acquired (H). r-EBUS, radial endobronchial ultrasound.

procedural CT (spontaneous breathing, deep inspiration at total lung capacity) and when the RAB procedure is performed (mechanical breathing under general anesthesia, possibly at functional residual capacity), “CT-to-body divergence” may occur, where the true location of a pulmonary lesion is not consistent with the virtual target. Therefore, even though successful localization to the target lesion may be demonstrated via feedback from the navigation system, the robotic bronchoscope may be off the target lesion. This is especially true when the target lesion is in the lower lobes, where atelectasis is more prevalent during general anesthesia and there is more diaphragmatic excursion. This has limited the accuracy for sampling smaller PPL when using any robotic or ENB technology.

For this reason, the location of the target lesion is typically confirmed with a second method of visualization. Advanced imaging can be used to verify the presence of “tool-in-lesion” prior to sampling. The use of advanced imaging techniques in addition to RAB for PPL sampling may have a role in improving diagnostic yield, but to date, no comparative study evaluated the additional benefit of adjuvant advanced imaging such as CBCT or augmented fluoroscopy. The use of multimodality approaches, including fluoroscopy and ROSE, during bronchoscopic evaluation of PPL has become common practice and has improved our approach and confidence for biopsy of PPL.

We highlight that CT-to-body divergence remains a pervasive problem across platforms using chest CTs performed during physiologic conditions to plan the pathways for PPL sampling under general anesthesia (30). In fact, a recent study using the Ion™ Platform has evaluated the prevalence of this issue (31). Divergence was defined as an overlap less than 10% between the target location on the pre-procedural CT and the target location during real-time mobile 3D imaging. Using this definition, divergence was identified in 50% of nodules, which increased to 60% when redefined on the basis of a distance of 10 mm between targets. This distinction was even more obvious when analyzed by location, where the median divergence ranged from 10 mm in the upper lobes to 21 mm in the lower lobes (31).

Radial EBUS

Radial EBUS is commonly used to confirm accurate localization of the target lesion and most studies showed increased diagnostic yield when an r-EBUS image is obtained, especially with a concentric view (3,17,21,23,32).

A meta-analysis of utilizing r-EBUS for PPL sampling which included 7,872 lesions showed an overall diagnostic yield of 70.6% (21) with a significant difference between concentric (79% yield) and eccentric view (52% yield). In a landmark study, Eberhardt and colleagues reported that the combined use of r-EBUS along with ENB improved diagnostic yield of up to 88% as compared with either technology alone (33). In non-robotic studies, the pattern of r-EBUS image affects diagnostic yield. In one study utilizing r-EBUS for PPL sampling, a higher diagnostic yield was noted when concentric r-EBUS views were obtained (84%) as compared with eccentric r-EBUS views (48%) (34). This seems intuitive as a concentric view suggest that the radial probe is surrounded by the lesion, while an eccentric view indicates that the probe is adjacent to the lesion. Whether this holds true for the RAB remains debatable. In our recently published RAB experience using the Monarch™ Platform, r-EBUS concentric views, eccentric views, and absent views were obtained in 37%, 45%, and 17%, respectively. The diagnostic accuracy was 85%, 84%, and 38% for concentric, eccentric, and absent r-EBUS views, respectively ($P < 0.001$) (11). Similarly, the BENEFIT trial also using the Monarch™ system, did not show a significant difference in diagnostic yields between concentric and eccentric r-EBUS views, with reported rates being 80.6% and 70%, respectively ($P = 0.502$) (4). This improvement in the diagnostic accuracy in patients with an eccentric r-EBUS view may be attributed by the increased peripheral visualization using the RAB platform and the ability to direct the biopsy tools towards the target lesion under direct visual guidance.

When using the r-EBUS probe, it is important to recognize that the orientation of the nodule on the r-EBUS display monitor does not represent the actual anatomic orientation in relationship to the target airway. Thus, when an eccentric r-EBUS view is obtained, the operator should define the position of the target lesion by evaluating the r-EBUS probe to airway wall interaction. This is done by moving the r-EBUS probe along different surfaces of the airway wall, while monitoring the pattern of the r-EBUS signal. When using the Monarch™ Platform, the r-EBUS probe can be moved onto different surfaces of the airway wall under continuous visualization. When using the Ion™ Platform, the vision probe must be removed before the r-EBUS probe can be inserted. Therefore, the r-EBUS articulation guide can be used to maneuver the r-EBUS probe in different positions systematically under fluoroscopic visualization to evaluate different surfaces of

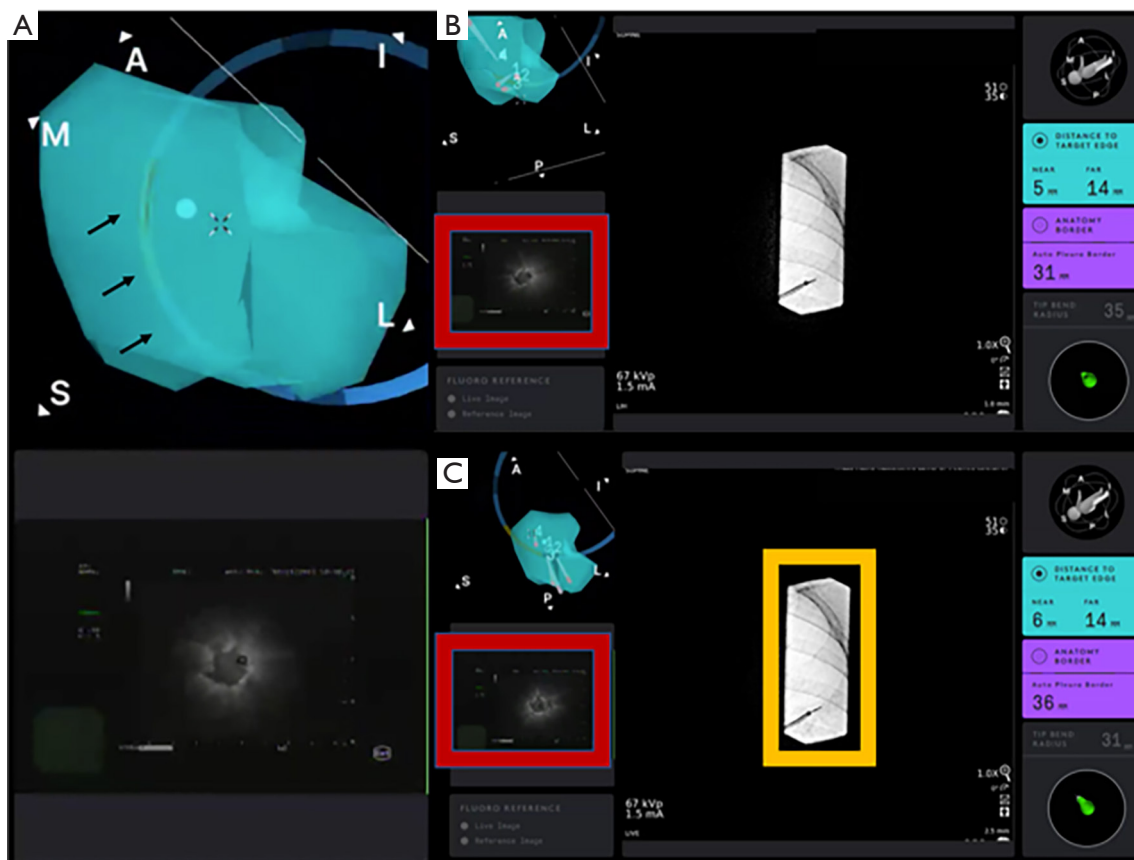


Figure 12 The articulation guide (black arrows) can be turned on to systemically guide the placement of the r-EBUS probe on different surfaces of the airway wall as the operator evaluates for the strongest r-EBUS signal (A). An eccentric r-EBUS view is obtained when the r-EBUS probe is advanced towards the lesion (red box) (B). Adjustments are made to the robotic catheter, by moving it anteriorly and superiorly as indicated by the endoluminal compass. A concentric view (red box) is obtained when r-EBUS probe is advanced towards the target lesion (C). Of note, the fluoroscopic projection is collimated to reduce the amount of radiation to the patient and procedure staff (yellow box). A, anterior; S, superior; M, medial; r-EBUS, radial endobronchial ultrasound.

the airway wall (Figure 12). Once the strongest r-EBUS signal is obtained, the bronchoscope working channel is aligned accordingly so that the operator can proceed with sampling.

Fluoroscopy

Due to the present technological limitations, real-time visualization of PPL sampling under direct ultrasound guidance is not yet possible. Therefore, fluoroscopy is often used to confirm the location of the bronchoscope and sampling instruments in relation to the pleura and pulmonary lesion during sampling, thus potentially increasing diagnostic yield and reducing the likelihood of

procedural related pneumothorax (35-42). Fluoroscopy remains highly utilized even with advanced guided bronchoscopic procedures for pulmonary nodule sampling (19,43,44). We will discuss the techniques the operators can use to reduce radiation exposure when using fluoroscopy in a subsequent section.

Augmented fluoroscopy

Tomosynthesis refers to a sweep arc performed around a patient's chest with continuous image acquisition to obtain multiple projections by using a conventional C-arm fluoroscopy machine. Augmented fluoroscopy utilizes tomosynthesis technology to offer local registration of the

peripheral target lesion and its relationship to a previously performed CT scan. This attempts to correct for CT-to-body divergence by allowing for updated confirmation of target lesion position and the ability to see the lesion in real-time with fluoroscopic imaging in three dimensions; allowing for fine adjustments of the RAB platforms to better align biopsy instruments with the target lesion, thus potentially increasing localization success and diagnostic yield (45-47). A retrospective study by Aboudara and colleagues demonstrated a 25% absolute increase in diagnostic yield (79%) when using this technology compared with using standard navigation alone (54%) (48). Several other studies have also demonstrated that augmented fluoroscopy may improve the diagnostic yield of sampling pulmonary lesions (45,46,49,50), but to date it is unclear whether this modality adds value to the existing RAB platforms in regard to diagnostic yield.

CBCT

CBCT is a technology that utilizes a compact CT system with a moving C-arm which can be used during bronchoscopy to provide real time feedback of the bronchoscope or tool location. The C-arm is swept in an arc around the patient's chest and obtains volumetric data during the procedure. The imaging can then be reviewed during the procedure to evaluate for bronchoscope, tool, and target locations and help the physician determine if adjustments are required to reach the target lesion. Pritchett and colleagues retrospectively reviewed data on 75 patients (93 lesions with a median size of 16 mm) where ENB combined with CBCT was used for PPL sampling and found that overall diagnostic yield was 83.7% (45). In a study of 20 patients, Casal and colleagues demonstrated a 25% absolute increase in diagnostic yield when sampling PPL with CBCT (47). A prospective study of 52 consecutive patients who underwent robotic bronchoscopy with the Ion™ Platform combined with CBCT for secondary confirmation, reported sensitivity of 84% for malignancy and overall diagnostic yield of 86% (13), but these studies included inflammation or other non-specific benign finding as true negative results.

In a different single-center, prospective, pilot study of Ion™ by Reisenauer *et al.*, 30 lesions with median size of 17.5 mm (median distance from pleura of 14.9 mm) were evaluated and tool-in-lesion was visualized at the time of the procedure in 29 lesions (96.7%). CBCT was used in all cases and the mean number of spins was 2.5

with mean fluoroscopy time of 8.7 min. There were no episodes of bleeding or pneumothorax (31). In a smaller study of 10 lesions in 5 patients using the Ion™ Platform in conjunction with the CIOS Mobile 3D spin, tool-in-lesion was confirmed in 90% of patients. The relationship between the biopsy tool and lesion was improved in 3 instances (30% of the time) after the subsequent redeployment of the tool, which was based on direct feedback from the intraoperative portable CT imaging (50). These studies suggest that tool-in-lesion confirmation is improved by adjuvant advanced imaging such as CBCT. We caution that subsegmental atelectasis can develop relatively fast during general anesthesia and in many cases (36%), it completely obscures the target lesion on CBCT (51). Thus, ultimately, in a patient-centered model of care, what matters is the diagnostic yield, when properly defined and not whether the tool is in what is thought to be the target lesion on advanced imaging, including CBCT.

Target lesion sampling

There are various instruments that have been used for lung nodule biopsy including needles, forceps, brushes, and occasionally cryobiopsy. Most studies use a multimodal approach. Comparison of biopsy modalities was evaluated in a *post-hoc* analysis of the NAVIGATE data in 2021 by Gildea *et al.* Biopsy modalities included forceps, aspirating needle, triple needle cytology brush, needle cytology brush, regular cytology brush, bronchoalveolar lavage, or core biopsy system. True positive rates were highest for forceps and aspirating needle (86.9% and 86.6%, respectively). Nearly all patients, however, had multiple tools applied during their procedure (52).

All studies published to date evaluating robotic bronchoscopy used needle biopsy as a standard for cytopathologic diagnosis. The aspirating needle provides the ability to traverse an airway wall in order to pierce a parenchymal lesion that has no endoluminal component. Withdrawal of the stylet slightly will apply a small amount of negative pressure without the application of a suction syringe (*Figure 13*). This “capillary pull” technique is equivalent to the suction technique for EBUS-TBNA, but has not been studied yet for PPL sampling (53). Suction, in our opinion, like in EBUS-TBNA, does not appear to alter specimen adequacy or diagnostic yield, and in practice may lead to more blood on the sample. The number of passes is usually dictated by adequacy of sample as determined by ROSE and the need for molecular and

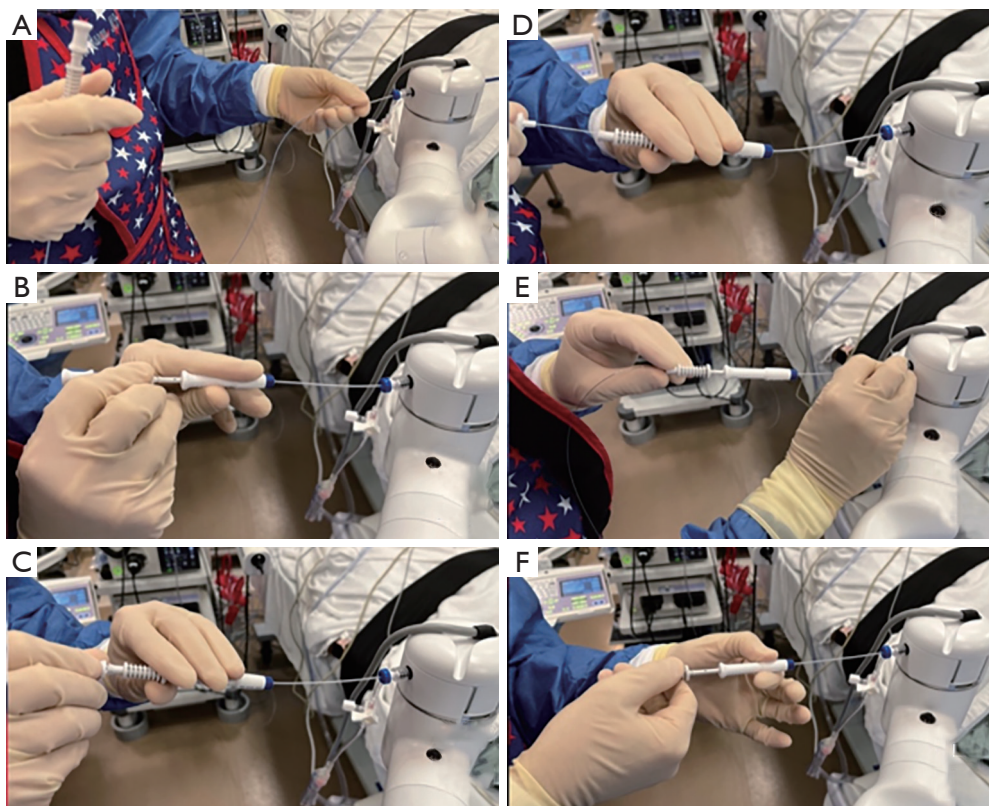


Figure 13 Example of stylet pull-back technique of needle aspiration. Needle system is advanced through working channel (A) until in position. Needle itself is advanced out of sheath into target with stylet slightly withdrawn (B). Stylet is advance to clear needle channel (C). Stylet is withdrawn several inches to establish negative pressure (D). Needle system is agitated forward and backward within target with stylet left partially withdrawn (E). Once sampling is completed, needle is withdrawn into system without manipulating stylet (F). Needle system is then withdrawn from working channel and specimen is deployed on slides for rapid on-site cytology evaluation.

immunohistochemistry testing. Unlike EBUS-TBNA, there is no data regarding the appropriate number of passes for robotic bronchoscopy. Thus, most sampling strategies start with 3–4 needle samplings and move on to forceps and maybe brushings. The exception to this may be with ground glass nodules, where forceps biopsy may be of higher utility compared to needle biopsy.

Micro-adjustments can be made on the robotic platform so that the robotic bronchoscope can be aimed towards the target area of the PPL utilizing multiple different visualization modalities. In the case of the Monarch™ system, the biopsy device may be aimed using white light visualization in addition to virtual or fluoroscopic confirmation. In the case of the Ion™ system, the vision probe is removed to provide a working channel, thus the biopsy device can be directed towards the target lesion using virtual or fluoroscopic confirmation only. The Ion™ system

allows for placement of biopsy markers on the virtual target to indicate areas of the PPL that was previously biopsied. Targeting different areas of the PPL at time of biopsy may improve tissue adequacy in conjunction with ROSE as it allows sampling of different portions of the target lesion, but this remains to be validated.

Specimen handling

Specimens obtained via needle aspiration or forceps biopsy should be processed in accordance with feedback from local pathology staff for optimal results. Additionally, training for proper specimen handling for the bronchoscopy technician or nurse is essential. Herein, we describe our method for specimen handling in the bronchoscopy suite.

For needle biopsy, the extended needle should be held over the glass slide and the stylet is advanced until a small

amount of solid material is expressed and then the slide is handed off to cytologist for slide preparation. Remainder of needle contents should be placed into CytoLyt™ container (a methanol-based, buffered cell wash solution) for cell block preparation. Forceps biopsy should be prepared as a TouchPrep; using gentle, brief pressure to apply the tissue to the glass slide before placing the tissue into formalin or CytoLyt™ (as decided by participating pathologist).

ROSE provides immediate feedback to the proceduralist. It may provide a firm diagnosis, confirm lesion sampling, or facilitate repositioning of the scope or tools to fine tune the biopsy site. It is worth noting that while ROSE has become a common practice in many centers, definitive evidence that it improves diagnostic yield for all peripheral bronchoscopy platforms is conflicting. A meta-analysis of 51 r-EBUS studies (N=7,601 patients), showed that the only factor associated with increased sensitivity for malignancy was the use of ROSE. Studies that used ROSE had a higher pooled sensitivity than studies that did not use ROSE (79% vs. 72%, with and without ROSE, respectively) (20). On the other hand, in the NAVIGATE study, the diagnostic yield was not affected by ROSE use (78.6% vs. 75.8%, with and without ROSE, respectively). In fact, ROSE extended the duration of the procedure. The median ENB-specific procedure time was 30 minutes with ROSE and 18 minutes without ROSE (19).

For robotic bronchoscopy, there are no trials comparing RAB with ROSE to RAB without ROSE, however the correlation between ROSE and final pathologic diagnosis while using RAB has been examined. The rate of agreement between the ROSE and the finalized pathologic interpretation was 89.9% using the Ion™ system in a tertiary cancer hospital (14). Using the Monarch™ system, we reported adequate specimens on ROSE in 56% of the cases that were diagnostic (11). Whether ROSE improves yield for RAB remains to be determined.

Diagnostic yield clarifications

Diagnostic yield is the most common metric by which a new bronchoscopic technology is being evaluated. However, there is currently no universally accepted or standardized definition or approach to measure diagnostic yield. Many studies vary in their approach which may lead to discrepancies in reported yields. Diagnoses usually fall in to 1 of 4 typical groups: malignancy, specific benign diagnosis, non-specific benign finding, and non-diagnostic (15).

The stricter definitions of diagnostic yield apply these

categorizations at the time of bronchoscopic biopsy (index procedure), as defined by the final pathologic diagnosis. Thus, the only cases that are termed diagnostic are those where malignancy is seen or have a specific benign diagnosis (e.g., specific infection or granulomas) at the time of biopsy. The more liberal definitions allow for inclusion of follow-up data for all non-malignant pathologic diagnoses. Thus, cases that are initially non-diagnostic, but are negative for malignancy when factoring in follow-up data, may be included as diagnostic when calculating yield. This is problematic as a biopsy of lung parenchyma or airway wall, thus non-representative of the target lesion, is considered diagnostic if the follow-up imaging or other biopsy confirmed resolution or a benign process. Definitions for each study are typically decided by the authors when analyzing the data, thus variations between a more strict or liberal approach are common. A summary of robotic diagnostic studies and their diagnostic yield definitions is provided in *Table 1*. A recent theoretical model was published showing how different definitions affect diagnostic yield. Three diagnostic yield methods (strict, intermediate, liberal) were applied to a hypothetical cohort of 1,000 patients. In this cohort, diagnostic yield ranged from 66.7% for strict to 88.9% for liberal, thus demonstrating the wide variation in diagnostic yield simply based on definition methodology alone (15).

As diagnostic yield definitions relate to robotic bronchoscopy, the BENEFIT study, the Agrawal *et al.* study using the Monarch™ system and the Kalchiem-Dekel *et al.* study using the Ion™ system had similar definitions of diagnostic yield and in fact showed similar diagnostic yields (4,11,14). In these studies, bronchoscopy specimens were reported in three categories: malignant, non-malignant, or non-diagnostic. Non-malignant diagnoses were termed diagnostic if later proven non-malignant on subsequent pathology (including excision/resection or repeat biopsy), lesion regressed, or was stable on follow-up imaging. In these studies, atypical cells were included as non-diagnostic, which is not the case in studies that used more liberal diagnostic yield definitions.

Preventing complications

There is a loss of tactile feedback when driving a robotic bronchoscope, which could theoretically lead to airway trauma followed by pneumothorax or bleeding. In addition, these complications can occur as a result of sampling. As mentioned earlier, it is important to pay close attention to

Table 1 Summary of recent robotic bronchoscopy studies using either the Monarch™ or Ion™ platforms

Study	Platform/No. of pts/follow-up	Navigation success/confirmation tool	Bronchus sign	Diagnostic yield definition	Tools/sampling technique	Adjuvant imaging	Reported diagnostic yield
Chaddha 2019, <i>BMC Pulm Med</i> (5)	Monarch/N =165/6 months	89% (r-EBUS)	64%	+/- (cons/max) [†]	Needle 100%; forceps 96%	r-EBUS, 2D fluoro	69–77%
Fielding 2019, <i>Respiration</i> (12)	Ion/N =29/6 months	97% (virtual); 93% (r-EBUS)	59%	--	Needle 97%; forceps 69%; Brush 76%; BAL/wash 86%	r-EBUS, 2D fluoro	79%
Chen 2021, <i>Chest</i> (4)	Monarch/N =55/12 months	96% (r-EBUS)	59%	++	Needle 100%; forceps ×3 [‡]	r-EBUS, 2D fluoro	74%
Benn 2021, <i>Lung</i> (13)	Ion/N =52/5–6 months	85% (virtual); 100% (CBCT)	46%	--	Needle 100%; forceps 76%	CBCT	86%
Kalchier-Dekel 2022, <i>Chest</i> (14)	Ion/N =131/12 months	99% (virtual)	63%	++	Needle 97%; forceps 32%	r-EBUS, 2D fluoro, 3D fluoro	82%
Agrawal 2022, <i>Ann Thorac Surg</i> (11)	Monarch/N =124/12 months	94% (virtual); 82% (r-EBUS)	75%	++	Needle 94%; forceps 94%	r-EBUS, 2D fluoro	77%

Diagnostic yield definitions are as follows: (--) specimen considered diagnostic if malignant or benign diagnosis, including inflammation. (-) Specimen considered diagnostic if malignant or benign diagnosis, including inflammation (cases with inflammation mostly show resolution or improvement, but incomplete follow-up). (+) Specimen considered diagnostic if malignant or benign diagnosis. Inflammation where follow-up was not available was considered as non-diagnostic. (++) Specimen considered diagnostic if malignant or specific non-malignant process explained presence of pulmonary lesion. Inflammation considered diagnostic if regression or resolution of lesion on follow-up imaging, if remains unchanged on follow-up imaging for >1 year, or confirmed on alternative sampling method (such as transthoracic or surgical biopsy). Inflammation without follow-up, atypical cells, normal pulmonary elements, and specimens with follow-up tests that confirmed a different diagnosis were considered as non-diagnostic. Cases with patients who pursued anti-neoplastic treatment without confirmed diagnosis, patients with new diagnosis of lung cancer via biopsy of another site, or in which definitive diagnosis was not established due to lack of follow-up were considered non-diagnostic. †, both conservative estimates (+) and maximal overall (-) diagnostic yield definitions were provided in this study; ‡, transbronchial forceps biopsy was used if findings from transbronchial needle aspiration was negative on ROSE on three occasions. BAL, bronchoalveolar lavage; 2D, two-dimensional; r-EBUS, radial endobronchial ultrasound; CBCT, cone beam computed tomography; Virtual, virtual target on the respective robotic navigation platform; N/A, data not available; ROSE, rapid on-site evaluation.

the visual displays that indicate the articulation tension, torque, and drive force surrounding the robotic scope when driving the robotic bronchoscope in order to minimize airway trauma. Published human trials have demonstrated overall safety of a RAB platform, with complication rates comparable to or lower than conventional bronchoscopy (4,5).

Bleeding

The incidence of significant airway bleeding as a result of transbronchial biopsy has been reported in 2–3% of cases (19,44,54,55). At the time of this writing, there are no published reports of airway bleeding from RAB sampling that have required the use of blood transfusion, open thoracotomy, or the use of endobronchial blockers.

However, bleeding may become more of a concern as this technology continues to develop and potentially be used for therapeutic ablation of inoperable malignant lesions.

To further decrease the risk of bleeding, we have modified our technique when using the Monarch™ Platform so that we keep the sheath wedged in the most distal segmental or sub-segmental airway possible. This way, if bleeding occurs during sampling, the blood will be drained through the scope into the suction tubing instead of spilling into the other segments causing hypoxemia (Figure 14). We also believe that this technique allows for clot formation in the peripheral airway. Similarly, when using the Ion™ Platform, the operator can advance and wedge the scope as distally as possible. During the rare situation of active bleeding, we typically apply cold saline via the bronchoscope followed by continuous suctioning

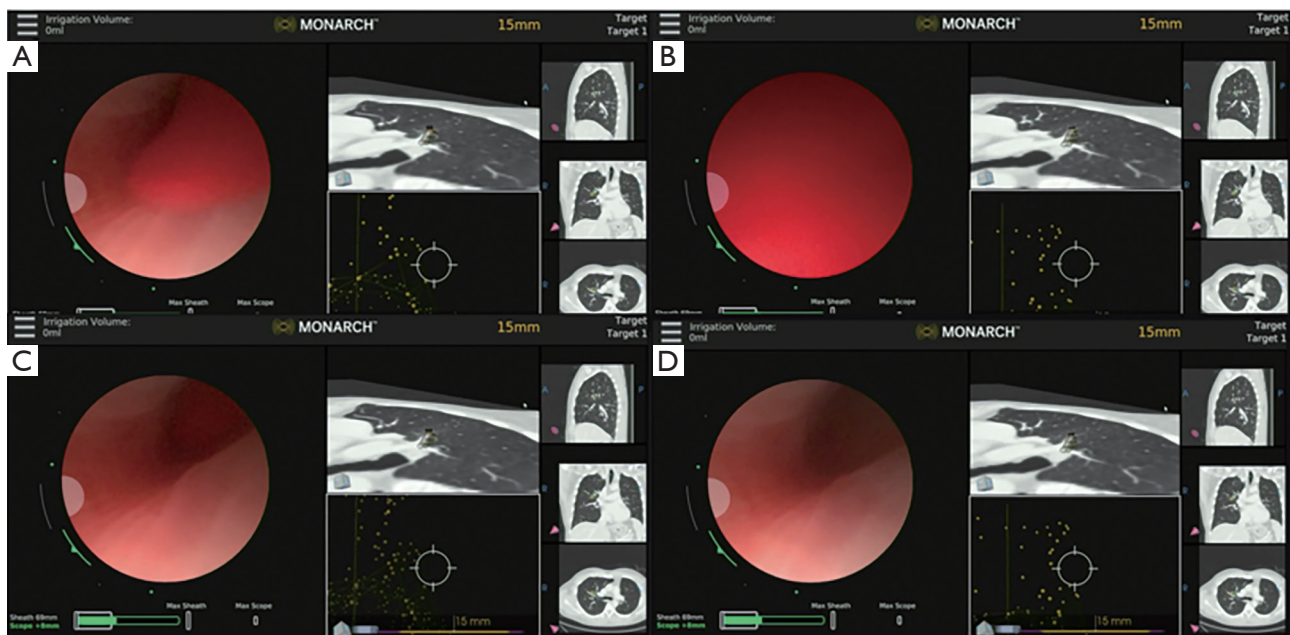


Figure 14 Airway bleeding is seen under continuous visualization on the Monarch™ Platform after biopsy of target lesion with grasping forceps (A). Since the sheath is wedged in the most distal segmental or sub-segmental airway possible, the blood will be drained through the scope into the suction tubing instead of spilling into the other segments causing hypoxemia (B). Iced saline is gently instilled via the working channel of the robotic bronchoscope to facilitate hemostasis (C). Hemostasis is achieved as no further bleeding is visualized on the robotic bronchoscope (D).

in a wedged position to collapse the distal airway and tamponade the bleed. With the Monarch™ system, we also inject 5–10 mL of cold saline at the end of the procedure while retrieving the robotic scope. If bleeding is visualized, the scope is kept in position and potentially colder saline is applied. Some operators have also used topical epinephrine (0.1 mg/mL × 4 mL) or tranexamic acid (250–500 mg), or endoscopic balloons for tamponade. Disconnecting and removing the robotic bronchoscope and introducing a therapeutic flexible bronchoscope could be done in cases of RAB-induced bleeding. We believe that the act of switching scopes does have the potential risk of losing a wedged position, anatomical orientation and potentially worsening the consequences of an otherwise isolated bleed (5). Our recently published experience with the Monarch™ Platform reported airway bleeding rate of 3.2%, which is comparable with PPL sampling with other technologies (11). With the Ion™ system, the airway bleeding rates have been reported in the range of 0–0.8% (12–14,31,56,57). The low rate of airway bleeding from PPL sampling may be related to the relatively low-pressure vascular system in the distal lung. This may also be due in part to the stability offered by the

RAB platforms and the ability to keep the robotic sheath wedged in the most distal segmental or sub-segmental airway possible.

Pneumothorax

Our recently published experience with the Monarch™ Platform demonstrated a pneumothorax rate of 1.6%, none of which required chest tube placement (11). The rate of pneumothorax in our study was relatively lower than other published studies involving PPL sampling with ENB or RAB (4,5,19,45). The pneumothorax rates in the BENEFIT trial were 3.7%; tube thoracoscopy was required in 1.9% (4). With the Ion™ system, the pneumothorax rates have been reported in the range of 0–3.8% (12,14,31,54,56,57).

The lower rate of pneumothorax may be related to stability of the RAB platform and the ability to wedge its sheath (Monarch™ system) in a segmental or even sub-segmental airway before the bronchoscope is advanced towards the target. This may prevent any airflow and positive pressure towards the target during ventilation at the time of biopsy and reduce the rate of pneumothorax even

if pleural injury occurs during sampling. In addition, once the sheath (Monarch™ system) or the scope (Ion™ system) are wedged in the target airway, the PEEP, tidal volume and pressure support settings can be normalized, potentially decreasing barotrauma in the area of sampling and thus decreasing the risk for pneumothorax. The injection of saline or blood patch created by post biopsy oozing could be responsible for the low pneumothorax rate. In fact, data from interventional radiology shows a significant reduction in the rate of pneumothorax if 1–4 mL of normal saline is injected while retrieving the needle during CT guided lung biopsies (58–60).

Radiation safety

The dose of radiation that bronchoscopy teams are exposed to has likely increased over the recent years as the use of fluoroscopically guided bronchoscopic procedures has increased. This is especially a concern since the bronchoscopist is often situated at the head of the patient adjacent to the mobile C-arm when operating the bronchoscope during conventional fluoroscopically guided bronchoscopic procedures. Many studies have demonstrated a dose-dependent effect between radiation exposure and adverse effects, suggesting occupational radiation exposure and different types of cancers are closely related (61–64). Interventional radiology and interventional cardiology procedures that use fluoroscopy have shown to cause brain tumors, hematologic malignancies, and lymphoma (65–70). Because of these stochastic effects, the US Nuclear Regulatory Commission (NRC) limits yearly occupational exposure to 50 mSv for the whole body, 150 mSv for the eye, and 500 mSv for the skin, hands, and feet (71,72). The International Commission on Radiological Protection (ICRP) Occupational Exposure Guidelines recommends a lower equivalent dose limit for the lens of the eye of 20 mSv averaged over five years with no single year exceeding 50 mSv (73).

When using fluoroscopy during RAB procedures, the operator should employ techniques to reduce radiation exposure from scattered radiation from the patient and X-ray tube leakage. For example, the image receptor should be lowered to keep the patient as close as possible to the receptor, and as far as possible from the X-ray source. Beam angulation should be avoided and collimation to the anatomic region of interest should be used when possible. Techniques in accordance with the ALARA principle (as low as reasonably achievable) and pulsed dose of fluoroscopy,

instead of continuous, should be used to minimize fluoroscopy time and maintain exposure to radiation as low as feasible during the procedure. Per standard of practice, all healthcare staff, including the bronchoscopists should be wearing appropriate protective shielding as recommended by ICRP and National Council on Radiation Protection and Measurements (NCRP). Particularly, non-lead composite aprons with knee-length front protection and thyroid shields, with lead equivalence of 0.35-mm thickness, should be worn. Protective lead glasses should also be worn by the bronchoscopist.

One particular advantage of using the RAB platforms is that the robotic bronchoscopy set up allows the bronchoscopist to operate the platform and sampling instruments at a further distance from the X-ray source as compared with conventional fluoroscopically guided bronchoscopy. By doubling the distance between the operator and the X-ray source, the radiation dose is reduced by a factor of 4. Therefore, by increasing the distance between the operator and the X-ray source from 0.5 to 2.0 meters, the radiation dose could be reduced by 16-fold (67,74). Whether these effects are translated into a lower radiation exposure dose in clinical practice remains to be determined.

Conclusions

Robotic bronchoscopy platforms have empowered bronchoscopists to access the periphery of the lung with more confidence and promising accuracy. We believe that vision, stability and farther reach of these modalities will continue to show improved diagnostic yields and safety. Our experience taught us that in addition to patient-related factors, careful planning, anesthesia settings, navigation, sampling and specimen handling techniques all affect diagnostic yield. CT-to-body divergence remains a problem across technologies and implementation of advanced imaging may mitigate it but confirmatory studies are needed.

Acknowledgments

Funding: None.

Footnote

Provenance and Peer Review: This article was commissioned by the Guest Editor (Calvin S. H. Ng) for the series “Lung

Cancer Management—The Next Decade” published in *Annals of Translational Medicine*. The article has undergone external peer review.

Peer Review File: Available at <https://atm.amegroups.com/article/view/10.21037/atm-22-3078/prf>

Conflicts of Interest: All authors have completed the ICMJE uniform disclosure form (available at <https://atm.amegroups.com/article/view/10.21037/atm-22-3078/coif>). The series “Lung Cancer Management—The Next Decade” was commissioned by the editorial office without any funding or sponsorship. EH receives consulting fees from Intuitive, Olympus, and Biodesix. SM receives consulting fees from Olympus, Boston Scientific, Pinnacle Biologics, Johnson and Johnson, ERBE, Biodesix and Cook Inc. for developing and delivering educational events. The authors have no other conflicts of interest to declare.

Ethical Statement: The authors are accountable for all aspects of the work in ensuring that questions related to the accuracy or integrity of any part of the work are appropriately investigated and resolved.

Open Access Statement: This is an Open Access article distributed in accordance with the Creative Commons Attribution-NonCommercial-NoDerivs 4.0 International License (CC BY-NC-ND 4.0), which permits the non-commercial replication and distribution of the article with the strict proviso that no changes or edits are made and the original work is properly cited (including links to both the formal publication through the relevant DOI and the license). See: <https://creativecommons.org/licenses/by-nc-nd/4.0/>.

References

1. Wahidi MM, Govert JA, Goudar RK, et al. Evidence for the treatment of patients with pulmonary nodules: when is it lung cancer?: ACCP evidence-based clinical practice guidelines (2nd edition). *Chest* 2007;132:94S-107S.
2. Sachdeva M, Ronaghi R, Mills PK, et al. Complications and Yield of Computed Tomography-Guided Transthoracic Core Needle Biopsy of Lung Nodules at a High-Volume Academic Center in an Endemic Coccidioidomycosis Area. *Lung* 2016;194:379-85.
3. Folch EE, Labarca G, Ospina-Delgado D, et al. Sensitivity and Safety of Electromagnetic Navigation Bronchoscopy for Lung Cancer Diagnosis: Systematic Review and Meta-analysis. *Chest* 2020;158:1753-69.
4. Chen AC, Pastis NJ Jr, Mahajan AK, et al. Robotic Bronchoscopy for Peripheral Pulmonary Lesions: A Multicenter Pilot and Feasibility Study (BENEFIT). *Chest* 2021;159:845-52.
5. Chaddha U, Kovacs SP, Manley C, et al. Robot-assisted bronchoscopy for pulmonary lesion diagnosis: results from the initial multicenter experience. *BMC Pulm Med* 2019;19:243.
6. Chen AC, Gillespie CT. Robotic Endoscopic Airway Challenge: REACH Assessment. *Ann Thorac Surg* 2018;106:293-7.
7. Chen AC, Pastis NJ, Machuzak MS, et al. Accuracy of a Robotic Endoscopic System in Cadaver Models with Simulated Tumor Targets: ACCESS Study. *Respiration* 2020;99:56-61.
8. Yarmus L, Akulian J, Wahidi M, et al. A Prospective Randomized Comparative Study of Three Guided Bronchoscopic Approaches for Investigating Pulmonary Nodules: The PRECISION-1 Study. *Chest* 2020;157:694-701.
9. Meza R, Jeon J, Toumazis I, et al. Evaluation of the Benefits and Harms of Lung Cancer Screening With Low-Dose Computed Tomography: Modeling Study for the US Preventive Services Task Force. *JAMA* 2021;325:988-97.
10. Rojas-Solano JR, Ugalde-Gamboa L, Machuzak M. Robotic Bronchoscopy for Diagnosis of Suspected Lung Cancer: A Feasibility Study. *J Bronchology Interv Pulmonol* 2018;25:168-75.
11. Agrawal A, Ho E, Chaddha U, et al. Factors Associated With Diagnostic Accuracy of Robotic Bronchoscopy With 12-Month Follow-up. *Ann Thorac Surg* 2023;115:1361-8.
12. Fielding DIK, Bashirzadeh F, Son JH, et al. First Human Use of a New Robotic-Assisted Fiber Optic Sensing Navigation System for Small Peripheral Pulmonary Nodules. *Respiration* 2019;98:142-50.
13. Benn BS, Romero AO, Lum M, et al. Robotic-Assisted Navigation Bronchoscopy as a Paradigm Shift in Peripheral Lung Access. *Lung* 2021;199:177-86.
14. Kalchiem-Dekel O, Connolly JG, Lin IH, et al. Shape-Sensing Robotic-Assisted Bronchoscopy in the Diagnosis of Pulmonary Parenchymal Lesions. *Chest* 2022;161:572-82.
15. Vachani A, Maldonado F, Laxmanan B, et al. The Impact of Alternative Approaches to Diagnostic Yield Calculation in Studies of Bronchoscopy. *Chest* 2022;161:1426-8.
16. Akulian JA, Molena D, Wahidi MM, et al. A Direct Comparative Study of Bronchoscopic Navigation Planning

- Platforms for Peripheral Lung Navigation: The ATLAS Study. *J Bronchology Interv Pulmonol* 2022;29:171-8.
17. Ali MS, Sethi J, Taneja A, et al. Computed Tomography Bronchus Sign and the Diagnostic Yield of Guided Bronchoscopy for Peripheral Pulmonary Lesions. A Systematic Review and Meta-Analysis. *Ann Am Thorac Soc* 2018;15:978-87.
 18. Seijo LM, de Torres JP, Lozano MD, et al. Diagnostic yield of electromagnetic navigation bronchoscopy is highly dependent on the presence of a Bronchus sign on CT imaging: results from a prospective study. *Chest* 2010;138:1316-21.
 19. Folch EE, Pritchett MA, Nead MA, et al. Electromagnetic Navigation Bronchoscopy for Peripheral Pulmonary Lesions: One-Year Results of the Prospective, Multicenter NAVIGATE Study. *J Thorac Oncol* 2019;14:445-58.
 20. Sainz Zuñiga PV, Vakili E, Molina S, et al. Sensitivity of Radial Endobronchial Ultrasound-Guided Bronchoscopy for Lung Cancer in Patients With Peripheral Pulmonary Lesions: An Updated Meta-analysis. *Chest* 2020;157:994-1011.
 21. Ali MS, Trick W, Mba BI, et al. Radial endobronchial ultrasound for the diagnosis of peripheral pulmonary lesions: A systematic review and meta-analysis. *Respirology* 2017;22:443-53.
 22. Brownback KR, Quijano F, Latham HE, et al. Electromagnetic navigational bronchoscopy in the diagnosis of lung lesions. *J Bronchology Interv Pulmonol* 2012;19:91-7.
 23. Hsia DW, Jensen KW, Curran-Everett D, et al. Diagnosis of lung nodules with peripheral/radial endobronchial ultrasound-guided transbronchial biopsy. *J Bronchology Interv Pulmonol* 2012;19:5-11.
 24. Hall SM, Hislop AA, Pierce CM, et al. Prenatal origins of human intrapulmonary arteries: formation and smooth muscle maturation. *Am J Respir Cell Mol Biol* 2000;23:194-203.
 25. LOOSLI CG, POTTER EL. Pre- and postnatal development of the respiratory portion of the human lung with special reference to the elastic fibers. *Am Rev Respir Dis* 1959;80:5-23.
 26. Ho E, Cho RJ, Keenan J, et al. The Feasibility of Using the "Vessel Sign" for Pre-Procedural Planning in Navigation Bronchoscopy for Peripheral Pulmonary Lesion Sampling: A Dual-Center Retrospective Study. *Am J Respir Crit Care Med* 2022;205:A3670.
 27. Sagar AS, Sabath BF, Eapen GA, et al. Incidence and Location of Atelectasis Developed During Bronchoscopy Under General Anesthesia: The I-LOCATE Trial. *Chest* 2020;158:2658-66.
 28. Salahuddin M, Sarkiss M, Sagar AS, et al. Ventilatory Strategy to Prevent Atelectasis During Bronchoscopy Under General Anesthesia: A Multicenter Randomized Controlled Trial (Ventilatory Strategy to Prevent Atelectasis -VESPA- Trial). *Chest* 2022;162:1393-401.
 29. Duggan M, Kavanagh BP. Pulmonary atelectasis: a pathogenic perioperative entity. *Anesthesiology* 2005;102:838-54.
 30. Pritchett MA, Bhadra K, Calcutt M, et al. Virtual or reality: divergence between preprocedural computed tomography scans and lung anatomy during guided bronchoscopy. *J Thorac Dis* 2020;12:1595-611.
 31. Reisenauer J, Duke JD, Kern R, et al. Combining Shape-Sensing Robotic Bronchoscopy With Mobile Three-Dimensional Imaging to Verify Tool-in-Lesion and Overcome Divergence: A Pilot Study. *Mayo Clin Proc Innov Qual Outcomes* 2022;6:177-85.
 32. Kurimoto N, Miyazawa T, Okimasa S, et al. Endobronchial ultrasonography using a guide sheath increases the ability to diagnose peripheral pulmonary lesions endoscopically. *Chest* 2004;126:959-65.
 33. Eberhardt R, Anantham D, Ernst A, et al. Multimodality bronchoscopic diagnosis of peripheral lung lesions: a randomized controlled trial. *Am J Respir Crit Care Med* 2007;176:36-41.
 34. Chen A, Chenna P, Loiselle A, et al. Radial probe endobronchial ultrasound for peripheral pulmonary lesions. A 5-year institutional experience. *Ann Am Thorac Soc* 2014;11:578-82.
 35. Rittirak W, Sompradeekul S. Diagnostic yield of fluoroscopy-guided transbronchial lung biopsy in non-endobronchial lung lesion. *J Med Assoc Thai* 2007;90 Suppl 2:68-73.
 36. Ahmad M, Livingston DR, Golish JA, et al. The safety of outpatient transbronchial biopsy. *Chest* 1986;90:403-5.
 37. Prigogine T, Schmerber J. Transbronchial lung biopsy without fluoroscopy. *Chest* 1987;92:187-8.
 38. Milman N, Faurischou P, Munch EP, et al. Transbronchial lung biopsy through the fibre optic bronchoscope. Results and complications in 452 examinations. *Respir Med* 1994;88:749-53.
 39. Rivera MP, Detterbeck F, Mehta AC, et al. Diagnosis of lung cancer: the guidelines. *Chest* 2003;123:129S-36S.
 40. Roth K, Hardie JA, Andreassen AH, et al. Predictors of diagnostic yield in bronchoscopy: a retrospective cohort study comparing different combinations of sampling

- techniques. *BMC Pulm Med* 2008;8:2.
41. Wallace JM, Deutsch AL. Flexible fiberoptic bronchoscopy and percutaneous needle lung aspiration for evaluating the solitary pulmonary nodule. *Chest* 1982;81:665-71.
 42. Triller N, Dimitrijevic J, Rozman A. A comparative study on endobronchial ultrasound-guided and fluoroscopic-guided transbronchial lung biopsy of peripheral pulmonary lesions. *Respir Med* 2011;105 Suppl 1:S74-7.
 43. Tanner NT, Yarmus L, Chen A, et al. Standard Bronchoscopy With Fluoroscopy vs Thin Bronchoscopy and Radial Endobronchial Ultrasound for Biopsy of Pulmonary Lesions: A Multicenter, Prospective, Randomized Trial. *Chest* 2018;154:1035-43.
 44. Ost DE, Ernst A, Lei X, et al. Diagnostic Yield and Complications of Bronchoscopy for Peripheral Lung Lesions. Results of the AQUIRE Registry. *Am J Respir Crit Care Med* 2016;193:68-77.
 45. Pritchett MA, Schampaert S, de Groot JAH, et al. Cone-Beam CT With Augmented Fluoroscopy Combined With Electromagnetic Navigation Bronchoscopy for Biopsy of Pulmonary Nodules. *J Bronchology Interv Pulmonol* 2018;25:274-82.
 46. Cicienia J, Bhadra K, Sethi S, et al. Augmented Fluoroscopy: A New and Novel Navigation Platform for Peripheral Bronchoscopy. *J Bronchology Interv Pulmonol* 2021;28:116-23.
 47. Casal RF, Sarkiss M, Jones AK, et al. Cone beam computed tomography-guided thin/ultrathin bronchoscopy for diagnosis of peripheral lung nodules: a prospective pilot study. *J Thorac Dis* 2018;10:6950-9.
 48. Aboudara M, Roller L, Rickman O, et al. Improved diagnostic yield for lung nodules with digital tomosynthesis-corrected navigational bronchoscopy: Initial experience with a novel adjunct. *Respirology* 2020;25:206-13.
 49. Hogarth DK. Use of augmented fluoroscopic imaging during diagnostic bronchoscopy. *Future Oncol* 2018;14:2247-52.
 50. Kalchiem-Dekel O, Fuentes P, Bott MJ, et al. Multiplanar 3D fluoroscopy redefines tool-lesion relationship during robotic-assisted bronchoscopy. *Respirology* 2021;26:120-3.
 51. Bhadra K, Setser RM, Condra W, et al. Lung Navigation Ventilation Protocol to Optimize Biopsy of Peripheral Lung Lesions. *J Bronchology Interv Pulmonol* 2022;29:7-17.
 52. Gildea TR, Folch EE, Khandhar SJ, et al. The Impact of Biopsy Tool Choice and Rapid On-Site Evaluation on Diagnostic Accuracy for Malignant Lesions in the Prospective: Multicenter NAVIGATE Study. *J Bronchology Interv Pulmonol* 2021;28:174-83.
 53. Kassirian S, Mitchell MA, McCormack DG, et al. Rapid On-site Evaluation (ROSE) in Capillary Pull Versus Suction Biopsy Technique With Endobronchial Ultrasound-transbronchial Needle Aspiration (EBUS-TBNA). *J Bronchology Interv Pulmonol* 2022;29:48-53.
 54. Pue CA, Pacht ER. Complications of fiberoptic bronchoscopy at a university hospital. *Chest* 1995;107:430-2.
 55. Mehta AC, Hood KL, Schwarz Y, et al. The Evolutional History of Electromagnetic Navigation Bronchoscopy: State of the Art. *Chest* 2018;154:935-47.
 56. Simoff MJ, Pritchett MA, Reisenauer JS, et al. Shape-sensing robotic-assisted bronchoscopy for pulmonary nodules: initial multicenter experience using the Ion™ Endoluminal System. *BMC Pulm Med* 2021;21:322.
 57. Reisenauer J, Simoff MJ, Pritchett MA, et al. Ion: Technology and Techniques for Shape-sensing Robotic-assisted Bronchoscopy. *Ann Thorac Surg* 2022;113:308-15.
 58. Billich C, Mucche R, Brenner G, et al. CT-guided lung biopsy: incidence of pneumothorax after instillation of NaCl into the biopsy track. *Eur Radiol* 2008;18:1146-52.
 59. Babu SB, Srinivasan S, Chung R, et al. Tract sealing with normal saline after percutaneous transthoracic lung biopsies. *J Med Imaging Radiat Oncol* 2020;64:211-4.
 60. Li Y, Du Y, Luo TY, et al. Usefulness of normal saline for sealing the needle track after CT-guided lung biopsy. *Clin Radiol* 2015;70:1192-7.
 61. Beir V. Health Effects of Exposure to Low Levels of Ionizing Radiation. In: National Research Council (US) Committee on the Biological Effects of Ionizing Radiation (BEIR V). Washington (DC): National Academies Press (US); 1990.
 62. Zablotska LB, Ashmore JP, Howe GR. Analysis of mortality among Canadian nuclear power industry workers after chronic low-dose exposure to ionizing radiation. *Radiat Res* 2004;161:633-41.
 63. Sont WN, Zielinski JM, Ashmore JP, et al. First analysis of cancer incidence and occupational radiation exposure based on the National Dose Registry of Canada. *Am J Epidemiol* 2001;153:309-18.
 64. Wang JX, Zhang LA, Li BX, et al. Cancer incidence and risk estimation among medical X-ray workers in China, 1950-1995. *Health Phys* 2002;82:455-66.
 65. Finkelstein MM. Is brain cancer an occupational disease of cardiologists? *Can J Cardiol* 1998;14:1385-8.
 66. Matanoski GM, Seltser R, Sartwell PE, et al. The

- current mortality rates of radiologists and other physician specialists: specific causes of death. *Am J Epidemiol* 1975;101:199-210.
67. Lee K, Lee KM, Park MS, et al. Measurements of surgeons' exposure to ionizing radiation dose during intraoperative use of C-arm fluoroscopy. *Spine (Phila Pa 1976)* 2012;37:1240-4.
 68. Hirshfeld JW Jr, Ferrari VA, Bengel FM, et al. 2018 ACC/HRS/NASCI/SCAI/SCCT Expert Consensus Document on Optimal Use of Ionizing Radiation in Cardiovascular Imaging-Best Practices for Safety and Effectiveness, Part 2: Radiological Equipment Operation, Dose-Sparing Methodologies, Patient and Medical Personnel Protection: A Report of the American College of Cardiology Task Force on Expert Consensus Decision Pathways. *J Am Coll Cardiol* 2018;71:2829-55.
 69. Perry BC, Ingraham CR, Stewart BK, et al. Monitoring and Follow-Up of High Radiation Dose Cases in Interventional Radiology. *Acad Radiol* 2019;26:163-9.
 70. Hadelsberg UP, Harel R. Hazards of Ionizing Radiation and its Impact on Spine Surgery. *World Neurosurg* 2016;92:353-9.
 71. Wrixon AD. New ICRP recommendations. *J Radiol Prot* 2008;28:161-8.
 72. National Council on Radiation Protection and Measurements. Limitation of Exposure to Ionizing Radiation. NCRP Report No. 116. Bethesda, MD: National Council on Radiation Protection and Measurements, 1993.
 73. Mao L, Liu T, Caracappa PF, et al. Influences of operator head posture and protective eyewear on eye lens doses in interventional radiology: A Monte Carlo Study. *Med Phys* 2019;46:2744-51.
 74. Schueler BA, Vrieze TJ, Bjarnason H, et al. An investigation of operator exposure in interventional radiology. *Radiographics* 2006;26:1533-41; discussion 1541.

Cite this article as: Ho E, Hedstrom G, Murgu S. Robotic bronchoscopy in diagnosing lung cancer—the evidence, tips and tricks: a clinical practice review. *Ann Transl Med* 2023;11(10):359. doi: 10.21037/atm-22-3078

Table S1 Summary of the search strategy used to identify articles which were referenced

Items	Specification
Date of search	June 1st, 2022
Databases and other sources searched	PubMed
Search terms used	Robotic bronchoscopy [MeSH] Robotic assisted bronchoscopy [MeSH] Navigational bronchoscopy [MeSH] Electromagnetic navigation [MeSH] Fluoroscopy [MeSH] Radial endobronchial ultrasound [MeSH] Transbronchial lung biopsy [MeSH] Peripheral pulmonary lesion [MeSH] Lung nodule [MeSH] Lung cancer [MeSH]
Timeframe	June 1st, 2002 to June 1st, 2022
Inclusion and exclusion criteria	Focus was placed on original papers and reviews in English about the use of robotic assisted bronchoscopy for peripheral pulmonary lesion sampling. It excluded articles that have no information about this topic of papers which we considered with low reliability
Selection process	It was conducted independently by E Ho and S Murgu; data selection is the intersection of the search of the two authors identified by reviewing reference lists of relevant publications
Any additional considerations, if applicable	Some papers were identified by reviewing reference lists of relevant publications